



Contents lists available at ScienceDirect

## Fungal Biology

journal homepage: [www.elsevier.com/locate/funbio](http://www.elsevier.com/locate/funbio)

## Lichen chemistry is concordant with multilocus gene genealogy in the genus *Cetrelia* (Parmeliaceae, Ascomycota)

Kristiina Mark<sup>a,b</sup>, Tiina Randlane<sup>a,\*</sup>, Göran Thor<sup>c</sup>, Jae-Seoun Hur<sup>d</sup>, Walter Obermayer<sup>e</sup>, Andres Saag<sup>a</sup>

<sup>a</sup> Institute of Ecology and Earth Sciences, University of Tartu, Lai 40, Tartu 51005, Estonia

<sup>b</sup> Institute of Agricultural and Environmental Sciences, Estonian University of Life Sciences, Kreutzwaldi 1, Tartu 51014, Estonia

<sup>c</sup> Swedish University of Agricultural Sciences, Uppsala, Sweden

<sup>d</sup> Korean Lichen Research Institute, Sunchon National University, 255 Jungang-Ro, South Korea

<sup>e</sup> Karl-Franzens-Universität, Graz, Austria

## ARTICLE INFO

## Article history:

Received 8 May 2018

Received in revised form

2 November 2018

Accepted 22 November 2018

Available online xxx

Corresponding Editor: Martin Grube

## Keywords:

Character evolution

Lichenized fungi

Molecular phylogeny

Secondary metabolites

Species delimitation

## ABSTRACT

The lichen genus *Cetrelia* represents a taxonomically interesting case where morphologically almost uniform populations differ considerably from each other chemically. Similar variation is not uncommon among lichenized fungi, but it is disputable whether such populations should be considered entities at the species level. Species boundaries in *Cetrelia* are traditionally delimited either as solely based on morphology or as combinations of morpho- and chemotypes. A dataset of four nuclear markers (ITS, IGS, Mcm7, RPB1) from 62 specimens, representing ten *Cetrelia* species, was analysed within Bayesian and maximum likelihood frameworks. Analyses recovered a well-resolved phylogeny where the traditional species generally were monophyletic, with the exception of *Cetrelia chicitae* and *Cetrelia pseudolivatorum*. Species delimitation analyses supported the distinction of 15 groups within the studied *Cetrelia* taxa, dividing three traditionally identified species into some species candidates. Chemotypes, distinguished according to the major medullary substance, clearly correlated with clades recovered within *Cetrelia*, while samples with the same reproductive mode were dispersed throughout the phylogenetic tree. Consequently, delimiting *Cetrelia* species based only on reproductive morphology is not supported phylogenetically. Character analyses suggest that chemical characters have been more consistent compared to reproductive mode and indicate that metabolite evolution in *Cetrelia* towards more complex substances is probable.

© 2018 British Mycological Society. Published by Elsevier Ltd. All rights reserved.

## 1. Introduction

Lichenized fungi form a morphologically, ecologically and evolutionary diverse group of fungi, mainly of Ascomycota, characterized by having mutualistic relationships with photoautotrophic partners. The lichen symbiosis has been highly successful with more than 19 000 currently accepted species of lichen-forming fungi, making up more than a quarter of the known ascomycetes (Lücking et al., 2017). Both adequate species delimitation and accurate identification of lichenized fungal species are essential not only for estimating biotic diversity, but also for managing and conserving natural resources, and for ecological research (Boluda

et al., 2019). The currently prevailing species concept, the general lineage concept (GLC), assumes that species represent independently evolving metapopulation lineages, while the specific operational criteria used for delimiting species may include different empirical properties associated with lineage formation, such as, e.g., morphological (sensu lato) characters, geographic range or monophyly, rather than a single indicator of species-level differentiation (Lumbsch and Leavitt, 2011; Carstens et al., 2013). Chemical traits, mainly the content of extracellular secondary metabolites within the thallus, have been widely used as discriminators at species level in lichen taxonomy since 1970s when a standardized thin layer chromatography (TLC) method was developed to identify the secondary compounds (Culberson, 1972; Culberson and Johnson, 1976). The application of chemicals as diagnostic to circumscribe species in lichen-forming fungi is generally accepted when chemical variants are linked to minor

\* Corresponding author. Fax: +372 737 6380.

E-mail address: [tiina.randlane@ut.ee](mailto:tiina.randlane@ut.ee) (T. Randlane).

morphological, ecological or distributional patterns (Elix and Stocker-Wörgötter, 2008; Cestaro et al., 2016). Thus, morphological and chemical character differences have traditionally served as proxies for identifying independently evolving lineages in lichenized fungi (Leavitt et al., 2013a), but this phenotype-based approach to species recognition has also been demonstrated in several cases to substantially misrepresent diversity, either underestimating the occurrence of cryptic species (Molina et al., 2011; Altermann et al., 2014; Boluda et al., 2016) or, on the contrary, overestimating the true diversity due to high levels of intra-specific morphological and chemical variation (Leavitt et al., 2011a, 2013b; Pino-Bodas et al., 2012; Velmala et al., 2014). The application of molecular data radically changed our ability to estimate evolutionary history and species delimitation in lichenized fungi. Although multilocus phylogenies are clearly preferred to single-gene trees when testing species boundaries (Lumbsch and Leavitt, 2011), the information derived from different genetic markers may be controversial, i.e. gene trees may appear incongruent with each other or with species trees (Maddison, 1997; Cummings et al., 2008) due to incomplete lineage sorting (Saag et al., 2014; Leavitt et al., 2016), interspecific hybridization, and a number of other reasons (Steinová et al., 2013). Multilocus coalescent-based species delimitation methods offer a substantial improvement over single gene trees or multilocus phylogenies using concatenated data by providing an effective tool for integrating multiple genetic loci from multiple individuals per species while modelling the coalescent gene histories within a shared species tree (Heled and Drummond, 2010; Leavitt et al., 2013b). Moreover, as phenotypical characters have been heavily utilized in traditional classifications, studying trait evolution along with molecular phylogenies serves as a useful tool for assessing the role of particular characters in forming chemical and morphological diversity of lichens (Divakar et al., 2013).

The family Parmeliaceae is among the most diverse lineages of lichenized fungi with almost 2800 currently accepted species, but appears also one of the most studied groups (e.g., Crespo et al., 2007; Divakar et al., 2015, 2017; Pizarro et al., 2018). Within Parmeliaceae, the lichen genus *Cetrelia* W.L. Culb. & C.F. Culb. represents a taxonomically interesting case where morphologically almost uniform populations differ considerably from each other chemically. Similar variation in secondary metabolite composition is not uncommon among lichenized fungi, observed, for example, in *Cladonia* (Timsina et al., 2014), *Pseudevernia* (Ferencova et al., 2010), *Ramalina* (Stocker-Wörgötter et al., 2004) and other genera, but it is disputable whether such populations should be considered entities at the species level (Lumbsch, 1998; Elix and Stocker-Wörgötter, 2008; Lumbsch and Leavitt, 2011).

*Cetrelia* was described by Culberson and Culberson (1968) who combined some species from *Cetraria* and *Parmelia* into a new genus, based mainly on chemical characters (atranorin in the upper cortex, and diverse secondary compounds in the medulla). The taxa in *Cetrelia* were previously considered 'cetrarioid' by reason of submarginal apothecia (Randlane et al., 1997), but are, however, phylogenetically closely related to *Xanthoparmelia* and other 'parmelioid' genera within the family Parmeliaceae (Crespo et al., 2007; Divakar et al., 2015). The genus is distributed mainly over the northern hemisphere, while the majority of the species are found in eastern Asia (Culberson and Culberson, 1968; Randlane and Saag, 1991, 2004).

The 18 currently accepted *Cetrelia* species (Randlane et al., 2013), listed in supplementary online material Table S1, are delimited using a combination of five morphotypes with six chemotypes (Randlane and Saag, 1991). Morphotypes are distinguished by the reproductive mode of lichens. The sorediate morphotype, characterized by the presence of (mainly) marginal

soralia, is the most widespread over the northern hemisphere, and taxonomically also the most discussed. The species in this group, *Cetrelia cetrarioides*, *Cetrelia chicitae*, *Cetrelia monachorum*, *Cetrelia olivetorum*, and *Cetrelia sayanensis*, are morphologically uniform, except for minute morphological differences of pseudocyphellae, soredia and soralia (Obermayer and Mayrhofer, 2007; Otnyukova et al., 2009). However, they differ considerably in their medullary chemistry. The chemotypes in *Cetrelia* represent constant medullary constituents that are all biosynthetically closely related orcinol-type depsides and depsidones (Culberson and Culberson, 1968). Each specimen produces a set of related substances — a chemosyndrome, where the same substances may be present in several species but in different quantities, acting either as a major or a minor compound — specific to its taxonomic affiliation (Culberson and Culberson, 1976). Depending on differing interpretations of this chemical diversity, some researchers have recognized only one species with four chemotypes in this group (e.g., Clerc, 2004; Santesson et al., 2004; Gilbert and Purvis, 2009), while others recognize the different chemotypes as separate species (e.g., Randlane and Saag, 1991; Obermayer and Mayrhofer, 2007; Wirth et al., 2013).

Despite controversial practises of species delimitation in *Cetrelia*, molecular studies have been scarce in the genus (Luo et al., 2007) and no phylogenetic evaluation of reproductive mode and thallus chemistry using comprehensive taxonomical research has been conducted. The main objectives of this study are: (i) to clarify the species delimitation in *Cetrelia* through molecular phylogenetic analyses; and (ii) to elucidate aspects of character evolution for lichen reproductive modes and major chemical compounds in this genus through evolutionary time.

## 2. Material and methods

### 2.1. Taxon sampling and identification

The dataset includes 58 samples of ten *Cetrelia* species collected mainly in Asia and, to a lesser extent, in Europe and North America (Table 1). Prior to sequencing, specimen identifications based on morphological and chemical characters (Culberson and Culberson, 1968; Randlane and Saag, 1991; Obermayer and Mayrhofer, 2007) were carried out. About 3–5 mg of visually uncontaminated lichen thallus of each specimen was soaked in acetone in a 2 ml tube for 3 h to extract the chemical substances for TLC. The solvent system A of the standardized TLC method (Orange et al., 2001) was used to separate lichen secondary compounds. The same piece of thallus was subsequently used for DNA extraction. Representatives from the genus *Xanthoparmelia* (Vain.) Hale were chosen as the outgroup for molecular analyses in accordance with Divakar et al. (2015).

### 2.2. Molecular methods

Thallus samples were disrupted in 2 ml microtubes with three stainless steel beads in a Mixer Mill MM 400 (Retsch) for three min at 30 Hz. Total genomic DNA was extracted using the Qiagen DNEasy Plant Mini Kit (QIAGEN, Hilden, Germany) following the manufacturer's Plant Tissue Mini Protocol and diluted in 80 µL elution buffer. DNA extractions were used for polymerase chain reactions (PCR) in a 12.5 µL of PCR Master Mix 2x (Fermentas). Four genomic markers were amplified: the entire internal transcribed spacer region (ITS), partial intergenic spacer region (IGS) from the nuclear ribosomal cistron, and fragments from two putative single-copy protein-coding genes, MCM7 and RPB1. Touch-down PCR following Lindblom and Ekman (2006) was used to amplify the ITS and IGS markers (IGS protocol of 66–56 °C). Protocols of Wedin et al. (2009) and Schmitt et al. (2009) in combination with a nested-PCR

**Table 1**

List of studied samples with their laboratory code, collection data and GenBank accession numbers for the sequences from analysed loci. Newly generated sequences are marked in bold. Sequence data for samples denoted with \* are mined from public database only.

Species	Laboratory code	Voucher info (locality, collection date, collector, collection number, herbarium)	Genbank accession number			
			ITS	IGS	MCM7	RPB1
<i>Cetrelia alaskana</i>	63769	USA: Alaska; 27.06.2004; Ahti, 63769 (TU)	<b>KX685843</b>	–	<b>KX685766</b>	<b>KX685731</b>
<i>C. alaskana</i>	CKM66	China: Tibet; 14.08.2000; Obermayer, 09925 (GZU)	<b>KX685844</b>	<b>KX685801</b>	–	<b>KX685732</b>
<i>C. alaskana</i>	CKM68	China: Tibet; 04.08.2000; Obermayer, 09485 (GZU)	<b>KX685845</b>	<b>KX685802</b>	–	–
<i>C. alaskana</i>	CKM70	China: Tibet; 14.08.2000; Obermayer, 09972 (GZU)	–	<b>KX685803</b>	–	–
<i>C. alaskana</i>	CKM72	China: Tibet; 13.08.2000; Obermayer, 09876 (GZU)	–	<b>KX685804</b>	–	–
<i>C. alaskana</i>	CKM74	Bhutan: Flor-Prov.; 26.07.2000; Miehe & Miehe, 00-242-20/04 (GZU)	–	<b>KX685805</b>	–	–
<i>C. alaskana</i>	CKM75	Bhutan: Flor-Prov.; 09.07.2000; Miehe & Miehe, 00-176-50/01 (GZU)	<b>KX685846</b>	–	–	–
<i>C. braunsiana</i>	25877	Japan: Hokkaido; 21.07.2010; Thor, 25877 (UPS, TU dupl.)	<b>KX685847</b>	<b>KX685806</b>	<b>KX685767</b>	<b>KX685733</b>
<i>C. braunsiana</i>	25985	Japan: Hokkaido; 23.07.2010; Thor, 25985 (UPS, TU dupl.)	<b>KX685848</b>	<b>KX685807</b>	<b>KX685768</b>	<b>KX685734</b>
<i>C. braunsiana</i>	28170	Japan: Honshu; 05.07.2012; Thor, 28170 (UPS, TU dupl.)	<b>KX685849</b>	<b>KX685808</b>	<b>KX685769</b>	<b>KX685735</b>
<i>C. braunsiana</i>	28444	Japan: Honshu; 10.07.2012; Thor, 28444 (UPS, TU dupl.)	<b>KX685850</b>	<b>KX685809</b>	<b>KX685770</b>	<b>KX685736</b>
<i>C. braunsiana*</i>	AT626	RU: Primorye; 26.09.1997; Kudryavtseva, 10983 (LD)	AF451760	–	–	–
<i>C. braunsiana</i>	CKM21	Russia: Primorye; 13.08.2010; Kuznetsova (LE)	<b>KX685851</b>	<b>KX685810</b>	<b>KX685771</b>	<b>KX685737</b>
<i>C. braunsiana*</i>	F000159	South Korea; Hur et al. (KoLABIC)	KM250170	–	–	–
<i>C. braunsiana*</i>	F005503	South Korea; Hur et al. (KoLABIC)	KM250171	–	–	–
<i>C. cetrarioides</i>	CKM13	Russia: Primorye; 11.08.2010; Kuznetsova (LE)	–	–	<b>KX685772</b>	–
<i>C. cetrarioides</i>	CKM41	Russia: Tverskaya; 23.08.2014; Notov (LE)	<b>KX685852</b>	<b>KX685811</b>	<b>KX685773</b>	<b>KX685738</b>
<i>C. cetrarioides</i>	CKM49	Russia: Tverskaya; 24.08.2014; Notov (LE)	<b>KX685853</b>	<b>KX685812</b>	<b>KX685774</b>	<b>KX685739</b>
<i>C. cetrarioides</i>	CKM51	Russia: Tverskaya; 08.08.2013; Notov (LE)	<b>KX685854</b>	<b>KX685813</b>	<b>KX685775</b>	<b>KX685740</b>
<i>C. cetrarioides</i>	CKM63	Russia: Chelyabinsk; 01.06.2009; Urbanavichene (LE)	<b>KX685855</b>	–	<b>KX685776</b>	<b>KX685741</b>
<i>C. cetrarioides</i>	CKM64	Russia: Chelyabinsk; 01.06.2009; Urbanavichene (LE)	–	<b>KX685814</b>	–	–
<i>C. cetrarioides*</i>	MAF15552	Spain: Asturias; 20.08.2003; Divakar (MAF-Lich 15552)	JN943844	–	KR995562	GU994692
<i>C. chicitae</i>	25865	Japan: Hokkaido; 21.07.2010; Thor, 25865 (UPS, TU dupl.)	<b>KX685856</b>	<b>KX685815</b>	<b>KX685777</b>	<b>KX685742</b>
<i>C. chicitae</i>	25922	Japan: Hokkaido; 22.07.2010; Thor, 25922 (UPS, TU dupl.)	<b>KX685857</b>	<b>KX685816</b>	<b>KX685778</b>	<b>KX685743</b>
<i>C. chicitae</i>	26063	Japan: Hokkaido; 23.07.2010; Thor, 26063 (UPS, TU dupl.)	<b>KX685858</b>	<b>KX685817</b>	<b>KX685779</b>	<b>KX685744</b>
<i>C. chicitae</i>	CKM07	Russia: Caucasus; 13.07.2013; Urbanavichene & Urbanavichus (LE)	<b>KX685859</b>	<b>KX685818</b>	<b>KX685780</b>	<b>KX685745</b>
<i>C. chicitae</i>	CKM15	Russia: Primorye; 14.08.2010; Kuznetsova (LE)	–	<b>KX685819</b>	–	–
<i>C. chicitae</i>	CKM18	Russia: Primorye; 13.08.2010; Kuznetsova (LE)	–	<b>KX685820</b>	–	–
<i>C. chicitae*</i>	F004688	South Korea; Hur et al. (KoLABIC)	KM250169	–	–	–
<i>C. japonica</i>	F016058	South Korea; 01.06.2012; Hur et al. (KoLABIC)	KM250166	<b>KX685822</b>	<b>KX685781</b>	<b>KX685746</b>
<i>C. japonica</i>	F016072	South Korea; 01.06.2012; Hur et al. (KoLABIC)	KM250168	<b>KX685823</b>	<b>KX685782</b>	<b>KX685747</b>
<i>C. japonica</i>	F016073	South Korea; 01.06.2012; Hur et al. (KoLABIC)	KM250167	<b>KX685824</b>	<b>KX685783</b>	<b>KX685748</b>
<i>C. japonica</i>	F016178	South Korea; 19.06.2012; Hur et al. (KoLABIC)	KM250165	<b>KX685825</b>	<b>KX685784</b>	<b>KX685749</b>
<i>C. japonica</i>	F016207	South Korea; 19.06.2012; Hur et al. (KoLABIC)	KM250164	<b>KX685826</b>	<b>KX685785</b>	<b>KX685750</b>
<i>C. japonica*</i>	Hur040790	South Korea; Hur et al.(KoLABIC)	EU142923	–	–	–
<i>C. japonica*</i>	Hur060828	South Korea; Hur et al.(KoLABIC)	EU142927	–	–	–
<i>C. monachorum</i>	24434	Japan: Hokkaido; 13.07.2010; Thor, 24434 (UPS, TU dupl.)	<b>KX685861</b>	<b>KX685827</b>	<b>KX685786</b>	<b>KX685751</b>
<i>C. monachorum</i>	CKM09	Russia: Caucasus; 14.07.2013; Urbanavichene & Urbanavichus (LE)	<b>KX685862</b>	<b>KX685828</b>	<b>KX685787</b>	<b>KX685752</b>
<i>C. monachorum</i>	CKM17	Russia: Primorye; 18.08.2010; Kuznetsova (LE)	<b>KX685863</b>	<b>KX685829</b>	<b>KX685788</b>	<b>KX685753</b>
<i>C. monachorum</i>	CKM31	Russia: Tverskaya; 09.11.2014; Notov (LE)	<b>KX685864</b>	<b>KX685830</b>	<b>KX685789</b>	<b>KX685754</b>
<i>C. monachorum</i>	CKM52	Russia: Tverskaya; 24.08.2014; Notov (LE)	<b>KX685865</b>	<b>KX685831</b>	<b>KX685790</b>	<b>KX685755</b>
<i>C. monachorum*</i>	MAF15507	China: Yunnan; 19.10.2002; Crespo et al. (MAF-Lich 15507)	JN943843	–	KR995563	GU994693
<i>C. olivetorum</i>	25016	Japan: Hokkaido; 15.07.2010; Thor, 25016 (UPS, TU dupl.)	<b>KX685866</b>	<b>KX685832</b>	<b>KX685791</b>	<b>KX685756</b>
<i>C. olivetorum</i>	28230	Japan: Honshu; 06.07.2012; Thor, 28230 (UPS, TU dupl.)	<b>KX685867</b>	<b>KX685833</b>	<b>KX685792</b>	<b>KX685757</b>
<i>C. olivetorum</i>	CKM01	Russia: Caucasus; 10.07.2013; Urbanavichene & Urbanavichus (LE)	<b>KX685868</b>	–	<b>KX685793</b>	<b>KX685758</b>
<i>C. olivetorum</i>	CKM04	Russia: Mordovia; 05.06.2014; Urbanavichene & Urbanavichus M3072 (LE)	<b>KX685869</b>	<b>KX685834</b>	<b>KX685794</b>	<b>KX685759</b>
<i>C. olivetorum</i>	CKM33	Russia: Tverskaya; 30.11.2014; Notov (LE)	<b>KX685870</b>	<b>KX685835</b>	<b>KX685795</b>	<b>KX685760</b>
<i>C. olivetorum</i>	CKM59	Estonia: Tartumaa; 30.08.2014; Randlane & Saag (TU)	<b>KX685871</b>	<b>KX685836</b>	<b>KX685796</b>	<b>KX685761</b>
<i>C. orientalis*</i>	AT406	Russia: Primorye; 29.08.1997; Skirina (LD-1062494)	AF451761	–	–	–
<i>C. pseudoliveterum</i>	F005458	South Korea; 27.10.2006; Hur et al. (KoLABIC)	KM250173	<b>KX685837</b>	<b>KX685797</b>	<b>KX685762</b>
<i>C. pseudoliveterum</i>	F007677	South Korea; 06.10.2007; Hur et al. (KoLABIC)	KM250172	<b>KX685838</b>	<b>KX685798</b>	<b>KX685763</b>
<i>C. pseudoliveterum*</i>	Hur030784	South Korea; Hur et al.(KoLABIC)	EU142922	–	–	–
<i>C. pseudoliveterum*</i>	Hur050176	South Korea; Hur et al.(KoLABIC)	EU142921	–	–	–
<i>C. pseudoliveterum*</i>	Hur060718	South Korea; Hur et al.(KoLABIC)	EU142930	–	–	–
<i>C. pseudoliveterum*</i>	Hur061074	South Korea; Hur et al.(KoLABIC)	EU142929	–	–	–
<i>C. pseudoliveterum*</i>	MAF15506	China: Yunnan; 19.10.2002; Crespo et al. (MAF-Lich 15506)	GU994548	–	KR995564	GU994694
<i>C. sanguinea</i>	CKM82	China: Tibet; 28.07.2000; Obermayer, 08854 (GZU)	–	<b>KX685839</b>	–	–
<i>C. sp. (perlatolic acid chemotype, morphotype not identifiable)</i>	CKM78	China: Tibet; 27.07.2000; Obermayer, 08041 (GZU)	<b>KX685860</b>	<b>KX685821</b>	–	–
<i>Xanthoparmelia chlorochroa*</i>	Leavitt55437	USA: North Dakota; Leavitt, 55437 (BRY-C)	HM578887	–	HM579688	KR995520
<i>Xanthoparmelia conspersa*</i>	MAF6793	Spain: Zamora; Blanco & Crespo (MAF-Lich 6793)	AY581096	–	–	EF092155
<i>Xanthoparmelia conspersa</i>	XAC01	Estonia: Läänemaa; 24.08.2015; Randlane (TU)	<b>KX685872</b>	<b>KX685840</b>	<b>KX685799</b>	<b>KX685764</b>
<i>Xanthoparmelia loxodes</i>	XAL01	Estonia: Läänemaa; 24.08.2015; Randlane (TU)	<b>KX685873</b>	<b>KX685841</b>	–	<b>KX685765</b>

method using inner primers were applied for RPB1 and MCM7, respectively. The second PCR step with internal primers (for ITS) or the same primers (for IGS) was also used to amplify the ribosomal genes of old samples with highly fragmented DNA. Primers used for PCR reactions, as well as for sequencing, and PCR temperature profiles are shown in Table 2. PCR products were visualized on a 1 % agarose gel mixed with ethidium bromide. Successful PCR products were purified with SAP/EXO treatment (Fermentas). Complementary strands of DNA were sequenced using the BigDye Terminator v3.1 Ready Reaction Cycle Sequencing Kit (Applied Biosystems, Foster City, CA, USA) on the ABI 3730xl DNA Analysers (Applied Biosystems) in the DNA Genotyping and Sequencing Core Facility of the Estonian Biocentre and Institute of Molecular and Cell Biology at the University of Tartu (Tartu, Estonia).

### 2.3. Single-locus and multilocus phylogenetic analyses

Sequence strands were assembled in Geneious v7.1 (Kearse et al., 2012). Contig sequence identities were confirmed in 'blastn' searches using the 'megaBLAST' algorithm against the NCBI nucleotide database (Altschul et al., 1990). The sequences were aligned in the program MAFFT v7 (Katoh and Standley, 2013), where the G-INS-i alignment algorithm (Katoh and Toh, 2008) with '1PAM/K = 2' scoring matrix was implemented for all loci.

Single-locus gene trees were reconstructed for all loci within a maximum likelihood (ML) framework using the program RAXML v7.3.1 (Stamatakis, 2006). Substitution models for each single-locus dataset were set to GTRGAMMA and branch supports were assessed using 1000 "fastbootstrap" replicates (Stamatakis et al., 2008). No strongly supported ( $\geq 70$  %) conflicts were found between the single-locus trees, and the datasets were concatenated for better phylogenetic resolution (Wiens, 1998).

The best partitioning scheme and evolution models for multilocus analyses were selected in PartitionFinder v1.1.1 (Lanfear et al., 2012) from BEAST models using corrected AIC model selection criterion and the greedy algorithm. We divided the dataset into a total of twelve blocks: first, into four blocks according to the loci, and then ITS and RPB1 were further divided into coding and noncoding parts (ITS was separated into partial 28S rRNA gene, ITS1, 5.8S rRNA gene, ITS2, and partial 18S rRNA gene, and RPB1 into three exons interrupted by two introns). PartitionFinder analysis resulted in two partitions, one constituting 1379 base pairs of protein-coding regions (18S, 5.8S, 28S, MCM7, and RPB1 exons 1, 2, and 3) evolving under TrN + I model, and another, including 935 base pairs of non-coding partitions (IGS, ITS1, ITS2, and RPB1 introns 1 and 2) where nucleotide substitution model was set to GTR + G.

ML and Bayesian (B/MCMC) analyses of the concatenated dataset were carried out in RAXML v7.3.1 and BEAST v1.8.3

(Drummond et al., 2012), respectively, in the CIPRES Science Gateway (Miller et al., 2010). The data were partitioned according to the PartitionFinder results. Two independent B/MCMC analyses were run, each for 200 million generations, sampling every 10 000th state. Convergence of the runs was assessed in Tracer v1.5 (Rambaut and Drummond, 2007). The fraction of 0.1 of each run was discarded before combining the remaining trees in LogCombiner v1.7.4 (Rambaut and Drummond, 2012a). A maximum clade credibility (MCC) tree, with posterior probabilities (PP) as branch support, was constructed in TreeAnnotator v1.7.4 (Rambaut and Drummond, 2012b) and visualized in FigTree v1.3.1 (Rambaut, 2009).

### 2.4. Species delimitation and phylogeny under the multispecies coalescent model

The multispecies coalescent model (MSC) provides a powerful framework for identifying putatively reproductively isolated lineages under ancestral polymorphism and gene tree-species tree conflicts. We estimated putative species in *Cetrelia* using the STACEY package (Jones, 2015) in BEAST v.2.5.1 (Bouckaert et al., 2014). STACEY allows each individual to be treated as a potential species and minimal split heights within the species or minimal cluster (SMC) trees are calculated under a birth-death-collapse prior. The prior is controlled by CollapseHeight ( $\epsilon$ ) parameter. We tested three different  $\epsilon$  values, 1.0E-3, 1.0E-4, and 1.0E-5, while the rest of the parameters were estimated and the BEAST analyses were set up as described for the concatenated data. Two different MCMC analyses with chain length of 200 million generations, sampling every 4000th state, were run for each CollapseHeight value. Convergence and effective sample size (ESS) were the highest for  $\epsilon = 1.0E-4$  and the SMC-trees from these two runs were further combined in LogCombiner, resampling every 8000th state and removing 10 % as a burn-in. An MCC tree with PP supports was constructed in TreeAnnotator and visualised in FigTree. Assignment of individuals into minimal clusters was assessed in SpeciesDelimitationAnalyzer (Jones et al., 2014) where CollapseHeight was set to  $\epsilon = 1.0E-4$  and the output with posterior probabilities of individuals belonging to the same minimal cluster was plotted as a similarity matrix in R v.3.3.2 (R Core Team, 2014). Minimal clusters or putative species were then validated in Bayesian Phylogenetics and Phylogeography (BPP) v3.1 using an unguided species delimitation method (Yang and Rannala, 2014) which implements Bayesian inference under the MSC model. For a large number of sequences and species, the applied reversible-jump Markov Chain Monte Carlo (rjMCMC) algorithm may encounter mixing problems (Yang and Rannala, 2010); thus, we reduced the number of specimens per minimal cluster to two and did not include outgroup taxa. Specimens with

**Table 2**  
Primers used for PCR amplification and sequencing of the studied loci.

Marker	Primer name	Primer sequence	Annealing temp. (C)	Reference
ITS	ITS1F	5'-CTT GGT CAT TTA GAG GAA GTA A-3'	62-52 (touchdown)	Gardes and Bruns (1993) White et al. (1990) Myllys et al. (1999) Lohtander et al. (1998)
	ITS4	5'-TCC CCG CTT ATT GAT ATG C-3'		
	ITS1LM	5'-GAA CCT GCG GAA GGA TCA TT-3'	68-58 (touchdown)	
	ITS2KL	5'-ATG CTT AAG TTC AGC GGG TA-3'		
IGS	IGSf	5'-TAG TGG CCG WTR GCT ATC ATT-3	62-52 (touchdown)	Wirtz et al. (2008) Wirtz et al. (2008)
	IGSr	5'-TGC ATG GCT TAA TCT TTG AG-3'		
MCM7	Mcm7-709for	5'-ACI MGI GTI TCV GAY GTH AAR CC-3'	56	Schmitt et al. (2009) Schmitt et al. (2009) Leavitt et al. (2011b) Leavitt et al. (2011b)
	Mcm7-1348rev	5'-GAY TTD GCI ACI CCI GGR TCW CCC AT-3'		
	LecMCM7f	5'-TAC CAN TGT GAT CGA TGY GG-3'	56	
	LecMCM7r	5'-GTC TCC RCG TAT TCG CAT NCC-3'		
RPB1	gRPB1-A for	5'-GAK TGT CCK GGW CAT TTT GG-3'	52-55	Matheny et al. (2002) Matheny et al. (2002) Mark et al. (2016) Saag et al. (2014)
	fRPB1-C rev	5'-CCN GCD ATN TCR TTR TCC ATR TA-3'		
	RPF-Usn3	5'-CTC GCA GTA CCY GTT TAC C-3'	55-49 (touchdown)	
	RPB1r-Cet2	5'-GCT GCT CAA ACT CRT TGA C-3'		

sequences from all four loci were preferred as representatives for the species candidates. Altogether 27 *Cetrelia* specimens, representing 15 minimal clusters as identified in STACEY, were analysed in BPP: alaskana1 (samples 63769, CKM75), alaskana2 (CKM68, CKM66), braunsiana (25877, CKM\_21), cetrarioides1 (MAF\_15552), cetrarioides2 (CKM\_63, CKM\_78), cetrarioides3 (CKM\_49, CKM\_51), chicitae1 (CKM\_07, 25865), chicitae2 (26063, 25922), chicitae3 (CKM\_15, CKM\_18), japonica (F016058, F016178), monachorum (CKM\_31, 24434), olivetorum (25016, CKM59), pseudolivetorum1 (F007677, F005458), pseudolivetorum2 (MAF\_15506) and sanguinea (XAC\_01). The population size parameters theta ( $\theta$ ) and divergence time parameter tau ( $\tau$ ) gamma priors were set to G (2, 400) and G (2, 200), corresponding to distribution means 0.005 and 0.01, respectively. Both rj algorithms 1 and 0 were run for 20,000 generations, sampling every second generation with a burn-in of 10 %. Alignment gaps and ambiguous nucleotides were used in likelihood calculations. Each analysis was run twice using different seeds and starting trees to confirm the consistency of the results, and the acceptance rates of the MCMC mixing were observed to stay around 30 %.

To estimate the species phylogeny and diversification times for *Cetrelia* populations, we reconstructed the coalescent-based and time-calibrated species tree in BEAST v1.7.4 (\*BEAST; Heled and Drummond, 2010). The eighteen species or minimal clusters (including three species from the outgroup) delimited in STACEY analyses were assigned as the putative candidate species. For rate-based node calibration, a fixed substitution rate of 0.00243 s/s/My (substitutions/site/million years) for the ITS marker was used. This estimate seems to prove relatively consistent estimate in Parmeliaceae in comparison to fossil-calibrated divergence estimates (Leavitt et al., 2015). The data were partitioned according to loci and four independent B/MCMC analyses were run in BEAST, each for 200 million generations, sampling every 10 000th state. An MCC tree with PP supports was visualized in FigTree where the time scale was set to represent millions of years and node bars 95 % highest posterior density (HPD) interval.

## 2.5. Character evolution analyses

We performed evolutionary analyses of characters including lichen major medullary compounds and reproductive modes by estimating probabilities of ancestral states, character consistency and rate of change, and by conducting statistical evaluation of different character evolution models. The major compounds in *Cetrelia* are all biosynthetically closely related orcinol-type molecules that differ in six structural features: oxidative coupling (i.e. the compound is either a depside or a depsidone), number of carbons in the A-ring chain, A-ring chain oxidation, number of carbons in the B-ring chain, B-ring chain oxidation, and methylation (Fig. 1 and supplementary online material Table S2; see also Culberson and Culberson, 1976 for further information). The different states of reproductive mode were identified based on the presence of specific reproductive structures, viz.: (1) vegetative reproduction by soredia, (2) vegetative reproduction by isidia or lobulae, or (3) sexual reproduction (i.e. presence of apothecia and/or pycnidia, and/or absence of specific vegetative propagules). Reproduction by thallus fragmentation is another type of vegetative reproduction where lichens lack any distinct reproductive structures. It is mostly found in terricolous lichens and in this genus might occur only in *Cetrelia alaskana*. However, we found sexual structures in four out of seven analysed *C. alaskana* specimens and decided to include specimens without vegetative reproductive structures in the third character state, i.e. sexual reproduction. Altogether, six chemical characters and one morphological character representing three reproductive modes were investigated. Binary coding was applied

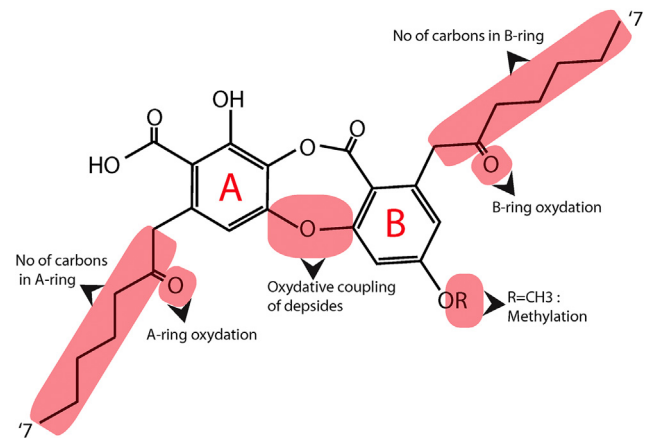


**Fig. 1.** Chemical formula of orcinol-type molecule, where two carbon rings are indicated as 'A' and 'B'. Structural elements (length of corresponding carbon tails, oxidation of a carbon tail, oxidative coupling of depsides, and methylation of the molecule) that differentiate between the variety of medullary substances produced in the genus *Cetrelia* are pointed out by red colour. (For interpretation of the references to colour in this figure legend, the reader is referred to the Web version of this article.)

to four metabolite structural characters: oxidative coupling, A-ring oxidation, number of carbons in the B-ring, and B-ring oxidation; and multistate coding to the rest three characters: number of carbons in the A-ring, methylation, and reproductive mode. The discrete states of all specimens investigated are listed in Table 3 as a character matrix for ancestral state analyses. States for the investigated characters were estimated for each ancestral node within the *Cetrelia* clade, altogether for 29 ancestral nodes, but not recorded nor reconstructed within the putative species or outgroup taxa. Most parsimonious states for each ancestral node, character consistency index (CI), character retention index (RI), number of parsimony steps between changes, and overall rate of change over the Bayesian majority rule consensus tree from the analysis of concatenated data were estimated in Mesquite v3.2 (Maddison and Maddison, 2017).

We reconstructed ancestral states for each character in Bayes-Traits v3 (Pagel et al., 2004; Pagel and Meade, 2006) using Multi-State method in ML and MCMC mode. A subset of 5000 BEAST trees, resampled at every 80 000th generation in LogCobMiner, were analysed to account for phylogenetic uncertainties. ML analyses were conducted for each character separately for 25 iterations and MCMC analyses for 200 million generations, sampling every 10 000th state, and removing 2 million generations as a burn-in. The asymmetrical Markov k-state 2 parameter model (AsymmMk), allowing differing rates for state changes, and uniform prior distributions between 0 and 100, were used. Average state probabilities over the analysed posterior distribution of trees were calculated for each state and rates of state change (Q).

We estimated the marginal likelihoods of different character history models for each character. Our null and the most simple model (M0) constrained all state changes to a single transition probability ( $Q_{0 \rightarrow 1} = Q_{1 \rightarrow 0}$ ), corresponding to the Mk1 model. A more complex, asymmetric model (Asym) allowed states to change in every direction in different rates or probabilities ( $Q_{0 \rightarrow 1} \neq Q_{1 \rightarrow 0}$ ), corresponding to the AsymmMk model. To evaluate complication or simplification of the secondary compounds over the evolutionary history we tested for two alternative models: a model of simplification (Cs) restricted addition of new chemical bonds in a compound (i.e. restriction for oxidative coupling, methylation, oxidation, addition of carbons;  $Q_{0 \rightarrow 1} = 0$ ,  $Q_{1 \rightarrow 2} = 0$ ,  $Q_{0 \rightarrow 2} = 0$ ); a model of complication (Cc) restricted loss of chemical bonds ( $Q_{1 \rightarrow 0} = 0$ ,  $Q_{2 \rightarrow 1} = 0$ ,  $Q_{2 \rightarrow 0} = 0$ ). To evaluate the linearity in

**Table 3**  
Character matrix for ancestral state reconstruction analyses. Transformation of states for characters (a–g): (a) 0 = no, 1 = yes; (b) 0 = 3, 1 = 5, 2 = 7; (c) 0 = no, 1 = yes; (d) 0 = 5, 1 = 7; (e) 0 = no, 1 = yes; (f) 0 = no, 1 = yes, 2 = both; (g) 0 = soredia, 1 = isidia/lobulatae, 2 = sexual structures and/or vegetative structures missing. Characters a–f represent structural features of the major compound in the chemotype.

Candidate species	Sample	(a) Oxidative coupling of depsides	(b) A-ring carbons	(c) A-ring oxidation	(d) B-ring carbons	(e) B-ring oxidation	(f) Methylation	(g) Reproductive mode
alaskana1	alaskana_63769_USA_Alaska	0	0	0	0	0	1	2
alaskana1	alaskana_CKM_75_Bhutan	0	0	0	0	0	1	2
alaskana2	alaskana_CKM_66_China	0	0	0	0	0	1	2
alaskana2	alaskana_CKM_68_China	0	0	0	0	0	1	2
alaskana2	alaskana_CKM_70_China	0	0	0	0	0	1	2
alaskana2	alaskana_CKM_72_China	0	0	0	0	0	1	2
alaskana2	alaskana_CKM_74_Bhutan	0	0	0	0	0	1	2
braunsiana	braunsiana_25877_Japan	1	2	1	1	1	2	0
braunsiana	braunsiana_25985_Japan	1	2	1	1	1	2	0
braunsiana	braunsiana_28170_Japan	1	2	1	1	1	2	0
braunsiana	braunsiana_28444_Japan	1	2	1	1	1	2	0
braunsiana	braunsiana_AF451760_RU_Primorye	1	2	1	1	1	2	0
braunsiana	braunsiana_CKM_21_RU_Primorye	1	2	1	1	1	2	0
braunsiana	braunsiana_KM250170_South_Korea	1	2	1	1	1	2	0
braunsiana	braunsiana_KM250171_South_Korea	1	2	1	1	1	2	0
ctrarioides1	ctrarioides_MAF_15552_Spain	0	1	0	0	0	1	0
ctrarioides2	ctrarioides_CKM_63_RU_Chelyabinsk	0	1	0	0	0	1	0
ctrarioides2	sp_CKM_78_China	0	1	0	0	0	1	2
ctrarioides3	ctrarioides_CKM_13_RU_Primorye	0	1	0	0	0	1	0
ctrarioides3	ctrarioides_CKM_41_RU_Tverskaya	0	1	0	0	0	1	0
ctrarioides3	ctrarioides_CKM_49_RU_Tverskaya	0	1	0	0	0	1	0
ctrarioides3	ctrarioides_CKM_51_RU_Tverskaya	0	1	0	0	0	1	0
ctrarioides3	ctrarioides_CKM_64_RU_Chelyabinsk	0	1	0	0	0	1	0
chicitaie1	chicitaie_25865_Japan	1	2	1	1	1	2	0
chicitaie1	chicitaie_CKM_07_RU_Kavkaz	1	2	1	1	1	2	0
chicitaie2	chicitaie_25922_Japan	1	2	1	1	1	2	0
chicitaie2	chicitaie_26063_Japan	1	2	1	1	1	2	0
chicitaie2	chicitaie_KM250169_South_Korea	1	2	1	1	1	2	0
chicitaie2	orientalis_AF451761_RU_Primorye	1	2	1	1	1	2	1
chicitaie3	chicitaie_CKM_15_RU_Primorye	1	2	1	1	1	2	0
chicitaie3	chicitaie_CKM_18_RU_Primorye	1	2	1	1	1	2	0
japonica	japonica_016058_South_Korea	0	2	1	1	1	1	1
japonica	japonica_016072_South_Korea	0	2	1	1	1	1	1
japonica	japonica_016073_South_Korea	0	2	1	1	1	1	1
japonica	japonica_016178_South_Korea	0	2	1	1	1	1	1
japonica	japonica_016207_South_Korea	0	2	1	1	1	1	1
japonica	japonica_EU142923_South_Korea	0	2	1	1	1	1	1
japonica	japonica_EU142927_South_Korea	0	2	1	1	1	1	1
monachorum	monachorum_24434_Japan	0	0	0	0	0	1	0
monachorum	monachorum_CKM_09_RU_Kavkaz	0	0	0	0	0	1	0
monachorum	monachorum_CKM_17_RU_Primorye	0	0	0	0	0	1	0
monachorum	monachorum_CKM_31_RU_Tverskaya	0	0	0	0	0	1	0
monachorum	monachorum_CKM_52_RU_Tverskaya	0	0	0	0	0	1	0
monachorum	olivetorum_MAF_15507_China	0	0	0	0	0	1	0
olivetorum	olivetorum_25016_Japan	0	1	0	1	1	0	0
olivetorum	olivetorum_28230_Japan	0	1	0	1	1	0	0
olivetorum	olivetorum_CKM_01_RU_Kavkaz	0	1	0	1	1	0	0
olivetorum	olivetorum_CKM_04_RU_Mordovia	0	1	0	1	1	0	0
olivetorum	olivetorum_CKM_33_RU_Tverskaya	0	1	0	1	1	0	0
olivetorum	olivetorum_CKM_59_Estonia	0	1	0	1	1	0	0
pseudolivetorum1	pseudolivetorum_005458_South_Korea	0	1	0	1	1	0	1
pseudolivetorum1	pseudolivetorum_007677_South_Korea	0	1	0	1	1	0	1
pseudolivetorum1	pseudolivetorum_EU142921_South_Korea	0	1	0	1	1	0	1
pseudolivetorum1	pseudolivetorum_EU142922_South_Korea	0	1	0	1	1	0	1
pseudolivetorum1	pseudolivetorum_EU142929_South_Korea	0	1	0	1	1	0	1
pseudolivetorum1	pseudolivetorum_EU142930_South_Korea	0	1	0	1	1	0	1
pseudolivetorum2	pseudolivetorum_MAF_15506_China	0	1	0	1	1	0	1
sanguinea	sanguinea_CKM_82_China	0	1	0	0	0	0	2
X_chlorochroa	Xanthoparmelia_chlorochroa_Leavitt_55437_USA_North_Dakota	?	?	?	?	?	?	?
X_conspersa	Xanthoparmelia_conspersa_XAC_01_Estonia	?	?	?	?	?	?	?
X_conspersa	Xanthoparmelia_conspersa_MAF_6793_Spain	?	?	?	?	?	?	?
X_loxodes	Xanthoparmelia_loxodes_XAL_01_Estonia	?	?	?	?	?	?	?

multistate chemical character evolution (number of carbons in A-ring and methylation) towards complication ( $Q_{0 \rightarrow 1} \rightarrow 2$ ) or simplification ( $Q_{2 \rightarrow 1} \rightarrow 0$ ) we tested a model of linearity (CI) by restricting two-fold jumps in structural complication or

simplification ( $Q_{0 \rightarrow 2} = 0, Q_{2 \rightarrow 0} = 0$ ). Finally, we aimed to evaluate the probabilities of state changes between sexual and vegetative reproduction by testing two alternatives: (1) a model that restricts species reproductive mode transition from sexual to vegetative

reproduction ( $R_v$ ;  $Q_{2 \rightarrow 1} = 0$ ,  $Q_{2 \rightarrow 0} = 0$ ) and (2) a model that restricts transition from mainly vegetative to sexual reproduction ( $R_s$ ;  $Q_{0 \rightarrow 2} = 0$ ,  $Q_{1 \rightarrow 2} = 0$ ).

We used a stepping stone sampler (Xie et al., 2011) in the MCMC analyses to estimate the marginal likelihood of different character evolution models. The stepping stone sampler was set to 200 with 5000 iterations at each step, with a beta distribution ( $\alpha = 0.4$ ,  $\beta = 1.0$ ); analyses were repeated for each character to ensure the estimates are stable. We applied the Bayes Factor (BF) test to evaluate the difference between the posterior distributions of the null model and an alternative model for each character, following the calculation  $\log BF = 2 [\log \text{marginL} (\text{complex model}) - \log \text{marginL} (\text{simple model})]$ . In interpretation of the BF values, we followed Kass and Raftery (1995: 777), with  $\log BF > 2$  suggesting positive evidence for the alternative model and rejecting the null model. Negative Bayes Factors support the null hypothesis over the alternative, more complicated model, with values  $\leq -2$  suggesting positive evidence for the null model and rejecting the alternative model.

### 3. Results

#### 3.1. Morpho- and chemotypes

The studied specimens represented three morphotypes defined according to the reproductive mode (Fig. 2): (1) sorediate taxa: *C. cetrarioides*, *C. chicitae*, *C. monachorum*, and *C. olivetorum*; (2) isidiate/lobulate taxa: *Cetrelia braunsiana*, *Cetrelia japonica*, *Cetrelia orientalis*, and *Cetrelia pseudolivetorum*; and (3) taxa without vegetative propagules: *C. alaskana*, and *Cetrelia sanguinea* (Table 4). Among the latter species, *C. sanguinea*, displaying pycnidia and emerging apothecia, obviously reproduces sexually. *C. alaskana*, although usually considered to reproduce vegetatively by thallus fragments, was placed into the same morphotype because sexual structures were recorded on some studied *C. alaskana* samples (see section 2.5. Character evolution analyses). A juvenile specimen CKM78 (perlatolic chemotype) had neither sexual structures nor vegetative propagules developed on the thallus, and remained thus unidentified (indicated as *C. sp.* in Table 1 and Fig. 3; could be assigned either to the sorediate *C. cetrarioides* or the sexual *Cetrelia delavayana*).

All six chemotypes accepted in the genus (Randlane and Saag, 1991) were identified among the sequenced samples, and categorized according to their major medullary substance(s) (Table 4): (1) imbricatic acid in *C. alaskana* and *C. monachorum*; (2) olivetoric acid in *C. olivetorum* and *C. pseudolivetorum*; (3) anziaic acid in *C. sanguinea*; (4) perlatolic acid in *C. cetrarioides* and specimen CKM78; (5) microphyllinic acid in *C. japonica*; (6) alectoronic and  $\alpha$ -collatolic acids in *C. braunsiana*, *C. chicitae* and *C. orientalis*. The species showed constant chemosyndromic profiles (containing, besides the major compounds, also minor substances) with no or little variation in the detected substances. The imbricatic acid chemotype usually included also perlatolic, anziaic, and 4-0-demethylimbricatic acids as minor compounds; the anziaic acid chemotype included additionally its methylated derivate – perlatolic acid; and the perlatolic acid chemotype included also 4-0-methylolivetoric and anziaic acids as minor substances.

#### 3.2. Molecular data

In total, 141 new sequences for 46 specimens were generated in this study (ITS = 31, IGS = 41, MCM7 = 34, and RPB1 = 35). Sequence data from 16 specimens were mined from the NCBI nucleotide database (accessed 25.01.2016), with morphology and chemistry checked by KM and TR. Newly generated sequences are

available under GenBank accession nos. KX685730–KX685873 and listed in Table 1. Single-locus trees and matrices are deposited in the TreeBase under study number S19683 (<https://treebase.org>). The full data matrix included 62 specimens and 2314 aligned nucleotides (ITS 569 bp, IGS 447 bp, MCM7 544 bp, RPB1 754 bp).

#### 3.3. Multilocus phylogeny of concatenated data

The majority-rule consensus tree based on the concatenated 4-locus data matrix is shown in Fig. 3, together with species attachments to morpho- and chemotypes. The genus *Cetrelia* was recovered as monophyletic with strong support. The traditionally circumscribed species *C. alaskana*, *C. japonica*, *C. monachorum* and *C. olivetorum* were recovered as monophyletic with maximum support, while the monophyly of *C. braunsiana* was strongly supported by one method (ML bootstrap support, BS = 76). Although the clade including *C. cetrarioides* was also monophyletic and strongly supported, the monophyly of *C. cetrarioides* remained unclear since the juvenile specimen CKM78 could belong to either *C. cetrarioides* or *C. delavayana*. Two traditionally circumscribed species, *C. chicitae* and *C. pseudolivetorum*, were polyphyletic in our analyses. Two further species, *C. sanguinea* and *C. orientalis*, were represented by a single specimen each; the former appearing as sister taxon to the *C. cetrarioides* clade, the latter included in the main clade of *C. chicitae*. *C. alaskana* and *C. monachorum*, both representing the imbricatic acid chemotype, were positioned at the base of the *Cetrelia* clade, while the rest of the taxa formed a more recently diverged monophyletic clade. The latter was divided into two strongly supported subclades, one containing the species *C. olivetorum* and *C. pseudolivetorum*, both representing the olivetoric acid chemotype, and the other including species from the rest of the four (anziaic, perlatolic, microphyllinic and alectoronic- $\alpha$ -collatolic acid) chemotypes. The fact that anziaic and perlatolic acids are biochemically closely related (perlatolic acid is the methylated derivate of anziaic acid) was reflected also in the multilocus phylogenies. Even though not strongly supported (Bayesian posterior probabilities, PP = 0.81; BP = 51), the two chemotypes formed a monophyletic group, including *C. sanguinea* (anziaic acid chemotype) and *C. cetrarioides* (perlatolic acid chemotype). The alectoronic and  $\alpha$ -collatolic acids chemotype formed a strongly supported monophyletic clade, containing two subclades that in general constituted *C. chicitae* and *C. braunsiana*. The microphyllinic acid chemotype, represented by *C. japonica*, also formed a strongly supported monophyletic clade, although its phylogenetic position remained unresolved in our study.

#### 3.4. Species delimitation

STACEY minimal cluster analyses resulted in a distribution mean of Nclusters = 17.9, averaged to 18 minimal clusters. These included three outgroup taxa and 15 monophyletic groups within the *Cetrelia* clade: 'monachorum' (PP = 1.00), 'alaskana1' (PP = 0.80), 'alaskana2' (PP = 0.76), 'pseudolivetorum1' (PP = 1.00), 'pseudolivetorum2' (PP = n.a.), 'olivetorum' (PP = 1.00), 'sanguinea' (PP = n.a.), 'cetrarioides1' (PP = n.a.), 'cetrarioides2' (PP = 0.72), 'cetrarioides3' (PP = 0.99), 'japonica' (PP = 1.00), 'chicitae1' (PP = 0.42), 'chicitae2' (PP = 0.27), 'chicitae3' (PP = 0.50), and 'braunsiana' (PP = 0.40) (Fig. 4).

BPP analyses supported the delimitation of the 15 groups within the genus *Cetrelia* with PP = 0.85. Even though not highly supported, the second best delimitation scenario with 14 groups and combining 'chicitae1' and 'chicitae2' received PP of only 0.12. All candidate species were delimited with PP  $\geq$  0.95, except for 'chicitae1', 'chicitae2', and 'chicitae3' (all PP = 0.94). Collapsing minimal groups were in every analysis supported with PP < 0.07.

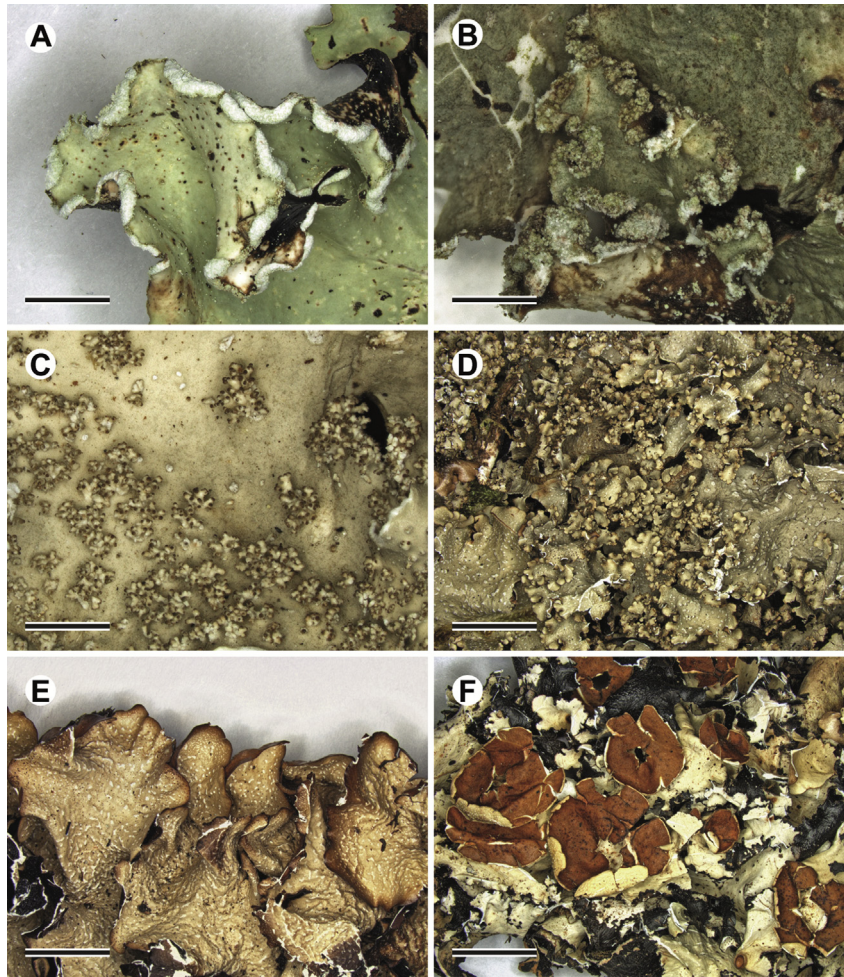


**Fig. 2.** The three morphotypes in *Cetrelia*: sorediate (A, B), isidiate and/or lobulate (C, D), and without vegetative propagules (E, F). Scale bars 2.8 mm (A), 1.3 mm (B, C), 6.4 mm (D), 5.4 mm (E), and 6.3 mm (F). Photographed specimens: (A) *Cetrelia olivetorum* DNA-CKM59, Randlane and Saag, Estonia (TU); (B) *C. chicitae* DNA-25878, Thor, Japan (UPS, TU); (C) *C. braunsiana*, Kärnefelt, Russia (LD-1040527); (D) *C. orientalis* DNA-AT406, Skirina, Russia (LD-1062494); (E) *C. alaskana* DNA-CKM66, Obermayer, China (GZU); (F) *C. sanguinea*, Indonesia, Sumatra (TU).

**Table 4**  
Traditionally delimited *Cetrelia* species, positioned according to their morphotype-chemotype combination, with morphological diagnostic characters. Analysed species are given in bold italics.

Morphotypes	Chemotypes; side chain lengths, oxidation (°), and oxidative cyclization (oxid. cycl.) of the major compounds					
	Imbricatic 3 + 5	Olivetoric 5 + 7°	Anziaic 5 + 5	Perlatolic 5 + 5	Microphyllinic 7°+7°	Alectronic + $\alpha$ -collatolic 7°+7°, oxyd. cycl.
Sorediate	<b><i>C. monachorum</i></b> soralia labriform, soredia coarse <i>C. sayanensis</i> soralia labriform to pustulate-capitate, soredia fine	<b><i>C. olivetorum</i></b> soralia labriform, soredia fine		<b><i>C. cetrarioides</i></b> soralia labriform, soredia fine		<b><i>C. chicitae</i></b> soralia labriform, soredia coarse
Isidiate and/or lobulate	<i>C. sinensis</i> lobules narrow to more broad, palmately divided	<b><i>C. pseudolivetorum</i></b> lobules narrow to more broad, multibranching	<i>C. isidiata</i> isidia globose to slightly branched and coralloid		<b><i>C. japonica</i></b> lobules narrow to more broad, multibranching	<b><i>C. braunsiana</i></b> isidia granular to coralloid <b><i>C. orientalis</i></b> lobules narrow to more broad, palmately divided <i>C. nuda</i> apothecia frequent, pseudocyphellae large
Without vegetative propagules	<i>C. collata</i> apothecia frequent, pseudocyphellae large <b><i>C. alaskana</i></b> apothecia rare, pseudocyphellae small	<i>C. davidiana</i> apothecia frequent, pseudocyphellae small	<b><i>C. sanguinea</i></b> apothecia frequent, pseudocyphellae small	<i>C. delavayana</i> apothecia frequent, pseudocyphellae small	<i>C. pseudocollata</i> apothecia frequent, pseudocyphellae large	<i>C. nuda</i> apothecia frequent, pseudocyphellae large



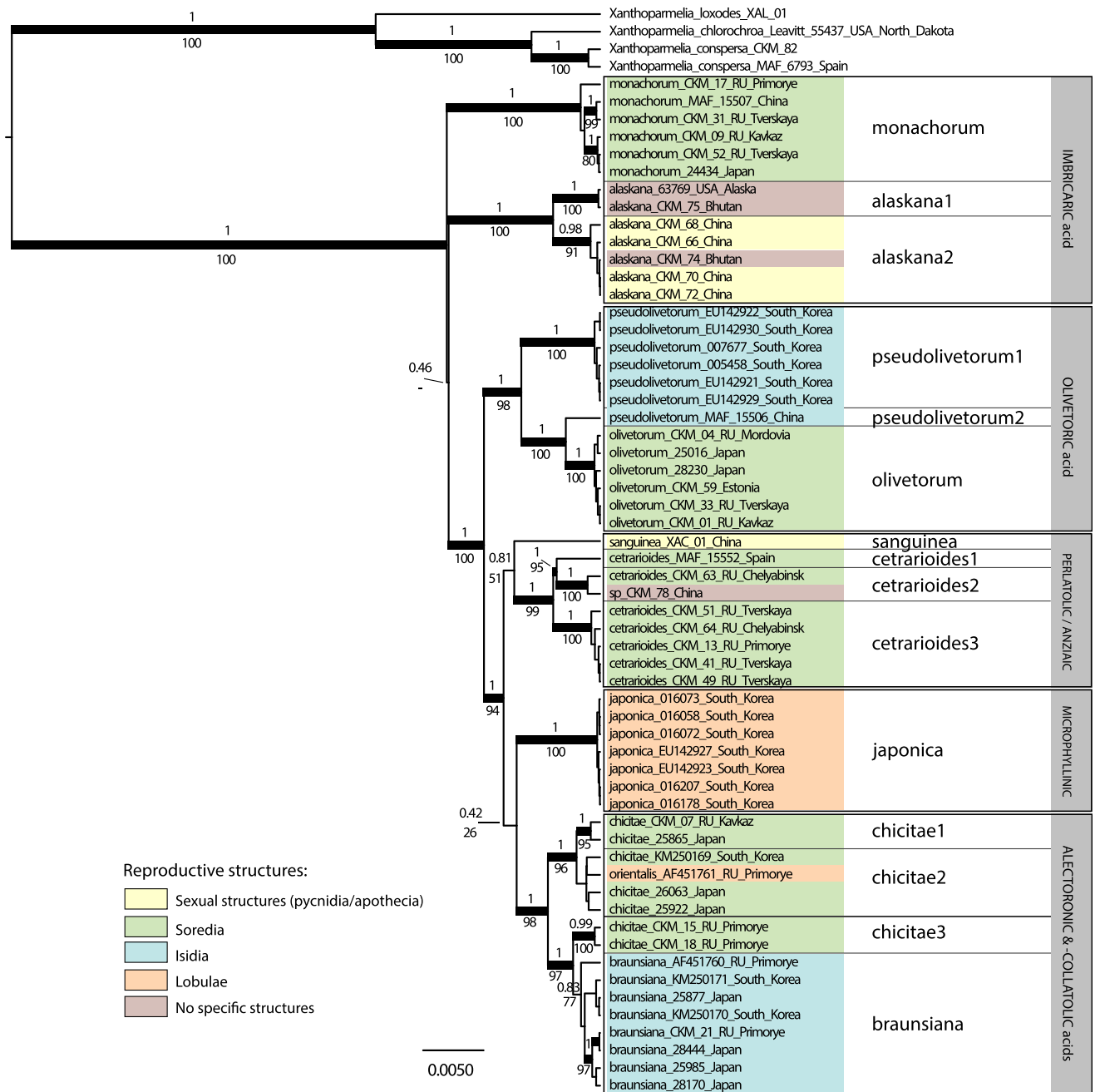


**Fig. 3.** The Bayesian majority-rule consensus tree of the studied ten *Cetrelia* species, based on four concatenated loci (ITS, IGS, Mcm7, RPB1), and inferred in BEAST. Posterior probabilities from the Bayesian concatenation analysis are given above, and nonparametric ML bootstrap supports from RAXML analysis below the branch. Branches leading to strongly supported nodes ( $\geq 95\%$  for BEAST and  $\geq 70\%$  for RAXML) are indicated in bold. Chemotypes are separated by squares and reproductive modes are indicated by colours. Scale bar shows the number of substitutions per site.

### 3.5. Coalescence-based species phylogenies and divergence time estimates

The structures and branch supports of the STACEY SMC-tree and the \*BEAST species tree were largely congruent (Fig. 4). Both of the trees corresponded to the concatenated multilocus phylogeny, showing the same topology and almost equivalent branch supports, with an exception in node 2 where \*BEAST estimated earlier divergence for *C. alaskana* (branching 2b), while STACEY and analyses of concatenated data showed *C. monachorum* diverging first (branching 2s). Neither of the topologies was highly supported in the analyses (PP support from \*BEAST, \*PP = 0.42, STACEY support,

S-PP = 0.63) and thus the tree remained unresolved in this node. The genus *Cetrelia* was monophyletic and highly supported in both of the coalescence-based phylogenies (\*PP = 1.00, S-PP = 1.00). The posterior probabilities of 14 \*BEAST nodes and 29 STACEY nodes are given on the Fig. 4A. The time-calibrated species tree analyses estimated the divergence time of *Cetrelia* to approximately  $22 \pm 7$  MYA, in the beginning of the Miocene. The species *C. alaskana* and *C. monachorum* showed the longest branches and appeared to be the oldest of the investigated *Cetrelia* species (20.6–22 MYA), while the youngest of the traditional species, *C. braunsiana*, dated back to  $2.9 \pm 3$  MYA, to the middle of the Pliocene. The estimated ages for each ancestral node are given in Fig. 4A.

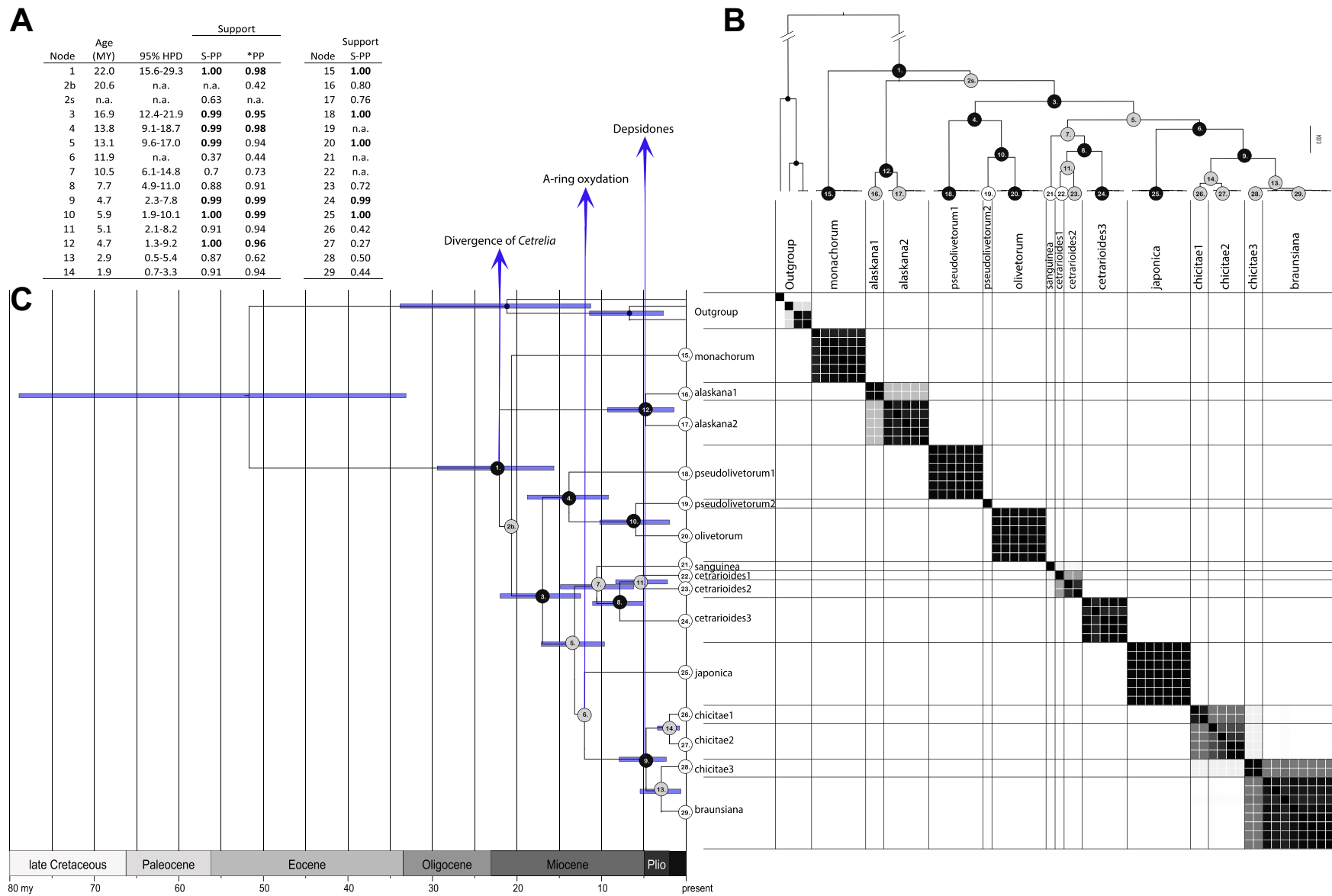


**Fig. 4.** STACEY species or minimal cluster delimitation similarity matrix together with its maximum clade credibility SMC-tree (B) and the rate-calibrated majority-rule consensus tree from the \*BEAST posterior sample of species trees (C). Node statistics [mean age, highest posterior density (HPD), and node posterior probabilities for the STACEY tree (S-PP) and \*BEAST tree (\*PP) are shown on the part (A). Similarity matrix squares represent posterior probabilities (white = 0, black = 1) of pairs of individuals to belong to the same minimal cluster. The lines in the matrix separate the 15 species or minimal clusters delimited within *Cetrelia* in STACEY analysis. The 29 nodes within the *Cetrelia* clade are numbered and ordered according to their mean divergence times; black circles representing strong node support ( $\geq 0.95$  either \*PP or S-PP), gray circles lower support ( $< 0.95$ ), and white circles on the \*BEAST tree for non-estimated nodes. 'Plio' marks for Pliocene, younger divisions are not shown.

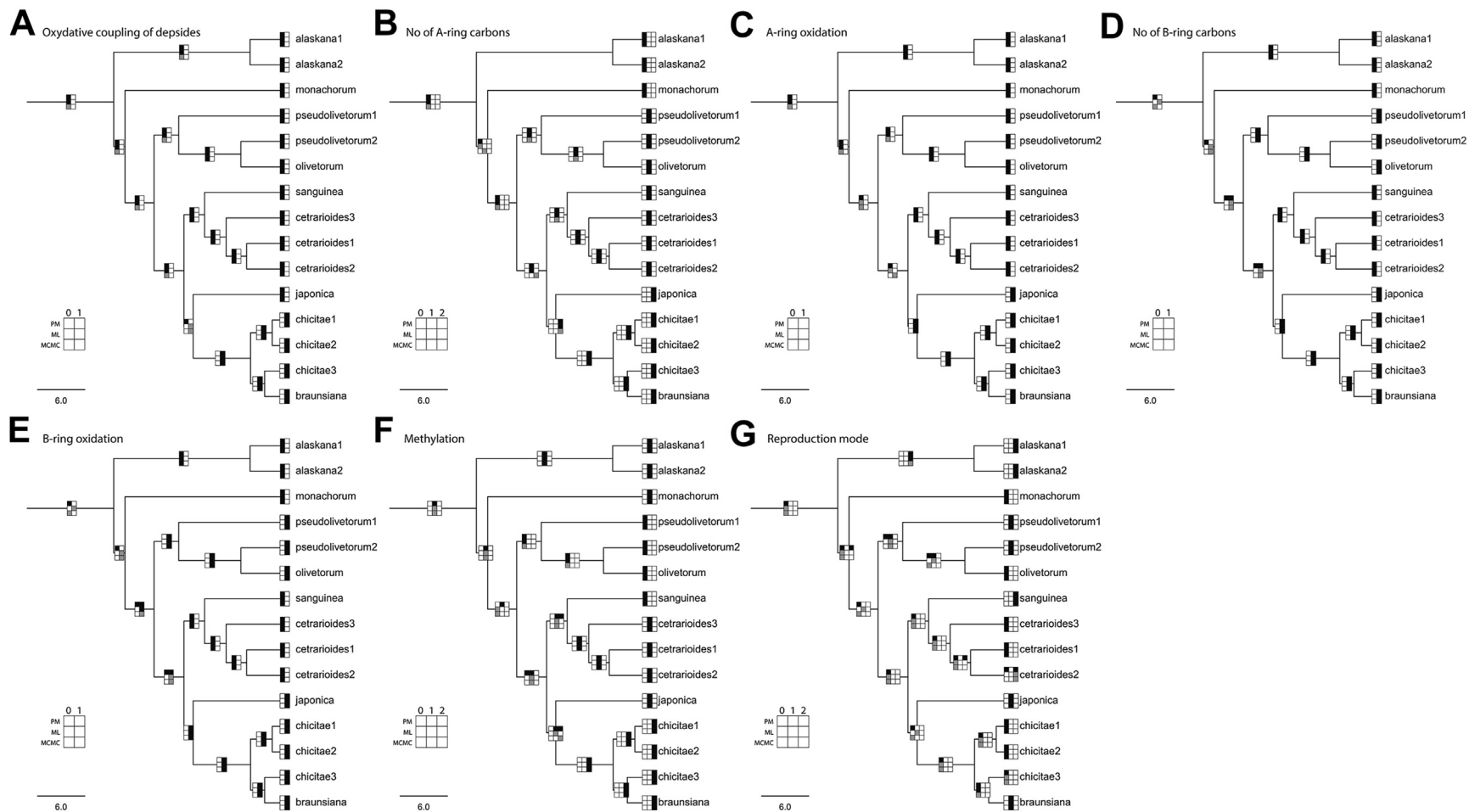


**Fig. 5.** Character states and state supports estimated in parsimony (PM), maximum likelihood (ML) and Markov Chain Monte Carlo (MCMC) methods for 29 ancestral nodes and seven characters (A–G), and plotted on the \*BEAST majority rule consensus tree. Shaded square (black in PM and black or gray in ML and MCMC) marks for state with highest support or most parsimonious. Black square in ML and MCMC mark for strong support ( $\geq 0.95$ ) and gray square for lower support ( $< 0.95$ ). For character state decoding see text or Table 3.

**Table 5**  
Character consistency indicators over the Bayesian concatenated multilocus majority-rule consensus tree.

Character	Character consistency index (CI)	Character retention index (RI)	Parsimony steps	Character change overall rate
Oxidative coupling of depsides	1.00	1.00	1	10.1 (bias: 0.43)
No. of A-ring carbons	1.00	1.00	2	16.5 (bias: 0.57)
A-ring oxidation	1.00	1.00	1	10.4 (bias: 0.60)
No. of B-ring carbons	0.50	0.95	2	21.3 (bias: 0.63)
B-ring oxidation	0.50	0.95	2	21.3 (bias: 0.63)
Methylation	0.67	0.96	3	20.5 (bias: 0.93)
Reproduction mode	0.29	0.77	7	59.6 (bias: 0.59)

### 3.6. Character analyses

Ancestral character states of 29 nodes were investigated, and the results (the most parsimonious states and the states with the highest likelihood from the ML and MCMC analyses) were plotted on the \*BEAST MCC species tree (Fig. 5). Most parsimonious states and the support for each node and character are given in supplementary online material Table S3. In general, all ancestral state estimation methods were mostly congruent, and no strongly supported conflicts between different estimates were found. Nodes representing older diversification events (e.g. node 1, 2, 3, etc.) generally received lower support values compared to the state estimates for putative species (nodes 15–29) where supports were usually >0.98. We found consistently strong support for (a) oxidative coupling of depsides (i.e. transitions from depsides to depsidones, with support in 28 nodes in ML and in 22 nodes in MCMC), (b) no. of A-ring carbons (in 28 and 22 nodes, respectively), (c) A-ring oxidation (in 26 and in 25 nodes, respectively), (d) no. of B-ring carbons (in 26 and in 25 nodes, respectively), and (e) B-ring oxidation (in 26 and in 25 nodes, respectively). Estimates with lowest likelihood were found for the reproduction mode, where none of the ancestral nodes preceding the putative species (i.e. nodes 1–14) could be assigned with a strongly supported ( $\geq 0.95$ ) state estimate from both analyses.

According to the current sampling, oxidative coupling of depsides has occurred only once (likelihood support, LS = 1.00, PP = 1.00; unambiguous character state change LS  $\geq 0.95$ ), at the time when the alectronic and  $\alpha$ -collatolic acids chemotype emerged (node 9; LS = 1.00, PP = 1.00). State changes in the number of carbons in the A-ring chain can be explained in two mutation steps: first, addition of two carbons at node 3 (LS = 0.98, PP = 0.72), and second, addition of two more carbons at node 6 (LS = 0.99, PP = 0.93). Number of carbons in the B-ring could be explained by two carbon-gain events, at nodes 4 (LS = 0.99, PP = 0.95) and 6 (LS = 0.99, PP = 0.97). A-ring oxidation has emerged once, at node 6 (LS = 1.00, BP = 0.98), while B-ring oxidation twice, at nodes 4 (LS = 0.99, PP = 0.95) and 6 (LS = 0.99, PP = 0.97).

We calculated consistency index, retention index, number of parsimony steps between changes and overall change rate over the Bayesian majority rule consensus tree for each investigated character (Table 5). Characters 'oxidative coupling of depsides', 'A-ring oxidation' and 'no. of A-ring carbons' showed the highest consistency indices with the maximum value (CI = 1; no homoplasy over the length of the tree). The least consistent character among the investigated traits was 'reproduction by soredia' (CI = 0.29); its overall change rate (59.6) was estimated at approximately six times higher than for the character with the lowest change rate ('oxidative coupling of depsides', 10.1). The distribution of reproductive modes on the Bayesian consensus tree was explained in seven parsimony steps. Reproduction by soredia was present in eight *Cetrelia* clades (i.e. 'monachorum', 'olivetorum', 'cetrarioides1', 'cetrarioides2', 'cetrarioides3', 'chicidae1', 'chicidae2', and 'chicidae3'). Reproduction by the corticated vegetative structures, isidia and lobules, has emerged almost equally frequently and were present in five different clades (i.e. 'pseudolivetorum1', 'pseudolivetorum2', 'japonica', 'chicidae2', and 'braunsiana'). The distribution of most chemical characters was explained in one or two parsimony steps, with the average character change overall rate being approximately 3.5 times lower than the rate for reproductive mode (16.7 and 59.6, respectively).

We compared the marginal likelihoods of different character evolution models to our null model (according to which all state changes were constrained to a single transition probability) in the Bayes Factor test (Table 6). Null models could not be rejected in favour of more complicated alternative model in any tests. Furthermore, in seven tests, values  $\leq -2 \log BF$  were recovered, suggesting positive evidence for the null model over the alternative model (rejecting the alternative model). These included: rejection of the simplification model (Cs) over the null hypothesis for (a) 'oxidative coupling of depsides' ( $\log BF = -6.17$ ), (b) 'no. of A-ring carbons' ( $\log BF = -5.05$ ), (c) 'A-ring oxidation' ( $\log BF = -4.56$ ), and (f) 'methylation' ( $\log BF = -5.52$ ). The complication model (Cc) was rejected for (f) 'methylation' ( $\log BF = -3.82$ ). AsymMk model was rejected for (b) 'no. of A-ring carbons' ( $\log BF = -2.42$ ).

**Table 6**  
Bayes Factor test results, where log BF values for each alternative model (Asym, asymmetric model; Cc, model of complication; Cs, model of simplification; Cl, model of linearity restricting two-fold jumps in structural complication or simplification; Rv, model restricting species reproductive mode transition from sexual to vegetative reproduction; Rs, model restricting transition from mainly vegetative to sexual reproduction) are given when compared to the null model [M0, all state changes constrained to a single transition probability ( $Q_{0 \rightarrow 1} = Q_{1 \rightarrow 0}$ ), where Q = character state change]. Values in bold indicate support in rejecting the alternative model over the null model.

Alternative models and character state change restrictions	Asym $Q_{0 \rightarrow 1} \neq Q_{1 \rightarrow 0}$	Cc $Q_{1 \rightarrow 0} = 0,$ $Q_{2 \rightarrow 1} = 0, Q_{2 \rightarrow 0} = 0$	Cs $Q_{0 \rightarrow 1} = 0,$ $Q_{1 \rightarrow 2} = 0, Q_{0 \rightarrow 2} = 0$	Cl $Q_{0 \rightarrow 2} = 0,$ $Q_{2 \rightarrow 0} = 0$	Rv $Q_{2 \rightarrow 1} = 0,$ $Q_{2 \rightarrow 0} = 0$	Rs $Q_{0 \rightarrow 2} = 0,$ $Q_{1 \rightarrow 2} = 0$
Character						
(a) Oxidative coupling	-0.50	-0.29	<b>-6.17</b>	n.a.	n.a.	n.a.
(b) No. of carbons in A-ring	<b>-2.42</b>	-0.64	<b>-5.05</b>	0.13	n.a.	n.a.
(c) A-ring oxidation	-0.48	-0.25	<b>-4.56</b>	n.a.	n.a.	n.a.
(d) No. of carbons in B-ring	-0.29	-1.68	-0.79	n.a.	n.a.	n.a.
(e) B-ring oxidation	-0.31	-1.60	-0.83	n.a.	n.a.	n.a.
(f) Methylation	-1.45	<b>-3.82</b>	<b>-5.52</b>	0.07	n.a.	n.a.
(g) Reproduction mode	-0.02	n.a.	n.a.	n.a.	1.86	<b>-10.60</b>

Reproduction mode change from sexual to vegetative (Rs) was rejected over the null model, suggesting that both changes, from sexual to vegetative and *vice versa*, are allowed ( $\log\text{BF} = -10.6$ ).

#### 4. Discussion

The Parmeliaceae have been the subject of many phylogenetic studies to elucidate the main clades and to delimit genera (e.g., Crespo et al., 2010; Amo de Paz et al., 2011; Divakar et al., 2015, 2017). The monophyly of the genus *Cetrelia* has so far not been questioned, a result supported by our study (Fig. 3). The estimated time of divergence obtained by our analyses within *Cetrelia*, approximately  $22 \pm 7$  MYA, is generally concordant with the earlier estimation of the mean age of the species divergence in this genus, 19.32 MYA, received by the temporal-based phylogeny for Parmeliaceae (Divakar et al., 2017, Fig. 1A). Species delimitation within the genus, on the contrary, has not been clarified up to now. The major problem of species delimitation in the genus *Cetrelia* is reflected by controversial practises of the interpretation of chemical variation: some researchers recognize different morphotypes as separate species, regardless of their medullary chemistry (e.g., Barbero et al., 1995; Santesson et al., 2004; Gilbert and Purvis, 2009), while others consider the combinations of morpho- and chemotypes as entities at the species level (e.g., Randlane and Saag, 1991; Kukwa and Motiejūnaitė, 2010; Wirth et al., 2013; Mishra and Upreti, 2015). In our multilocus analyses, the interspecific structure within the *Cetrelia* phylogeny, in both the concatenated tree (Fig. 3) and the coalescence-based species tree (Fig. 4), was generally concordant with chemotypic data. Samples of the same chemotype clustered together, while samples with the same reproductive mode, i.e. morphotypes, were dispersed throughout the phylogenetic tree. This clearly demonstrates that delimiting *Cetrelia* species based only on reproductive morphology is not supported phylogenetically. Another practise, discriminating traditionally circumscribed *Cetrelia* species by combining morphotypes and chemotypes, is supported in this research for the majority of studied taxa, while species boundaries of *C. chicitae*, *C. orientalis*, and *C. pseudolivetorum* remained unclear.

When species boundaries were estimated under the MSC model using genetic data, four traditional species, *C. alaskana*, *C. cetrarioides*, *C. chicitae*, and *C. pseudolivetorum*, were split with high support into multiple putative species (Fig. 4). However, no morphological, ecological, or distributional data contributed to the delimitation of these putative species, indicating that they constituted cryptic species. Furthermore, it has been shown that the MSC model is not able to distinguish between structure associated with population isolation and species boundaries (Sukumaran and Knowles, 2017), suggesting that the delimited cryptic species could also represent populations undergoing divergence, which could result in speciation given a cessation of gene flow. For this reason, here with the current dataset, we do not propose any taxonomic changes.

Character evolution analysis has been applied to investigate the features of both chemical and morphological evolution in *Cetrelia* (this study), and earlier in different groups of lichenized fungi (e.g., Buschbom and Barker, 2006; Lumbsch et al., 2006), including other Parmeliaceae (Divakar et al., 2013). If chemical characters are analysed, usually the presence or absence of a specific compound is under investigation. In our study, we looked at the structure and complexity of the compounds because the direction of chemical evolution in *Cetrelia* was of interest. Progressive chemical evolution towards shorter side chains, as proposed by Culberson and Culberson (1968, 1976), and Randlane and Saag (1991), appeared improbable in the light of our data. Bayes Factor comparison rejected the character simplification over the null model in four out

of six investigated characters of compound structure (Table 6). Character evolution analysis and comparison of the most parsimonious states at the node indicating the beginning of divergence within *Cetrelia* (node 1, dating approximately to  $22 \pm 7$  MYA) with the node which indicates the origin for the most recent chemotype (with alecoronic and  $\alpha$ -collatolic acids; node 9, ca  $4.7 \pm 3$  MYA), suggested the direction of evolution in chemical characters in *Cetrelia* towards more complex substances.

Investigating morphological evolution in *Cetrelia*, we focused on reproductive characters. The ancestral states for reproductive mode were, in general, weakly supported (Table S3) and average character change overall rate of reproductive characters was approximately 3.5 times higher than the average of chemical characters (Table 5). Observed elevated character inconsistency in the evolution of morphological traits could be caused by several factors, potentially including stronger selective pressure on reproductive mode, or as a plastic response to an ecological niche, compared to secondary metabolites, which are presumably not directly involved in the growth, development and reproduction of lichens (Nash, 2008).

These results are related to the concept of “species pairs” according to which a sexually reproducing species, called the “primary species”, often has a closely related asexual counterpart, termed the “secondary species”, with similar morphology and same secondary chemistry (Poelt, 1970; Crespo and Pérez-Ortega, 2009; Tripp, 2016). Poelt (1970) suggested that largely asexual “secondary species” have evolved by a one-time event from exclusively sexual “primary species”. Bowler and Rundel (1975) developed this hypothesis by assuming that chemical diversification occurred prior to the development of secondary, asexual (sorediate and isidiate) reproductive mechanisms. Culberson and Culberson (1976) presented a theory of parallel morphological and chemical evolution in *Cetrelia* according to which the chemical differentiation need not invariably precede morphological evolution but both differentiation processes could occur in parallel as most of the chemical variation in this genus could have arisen by somatic loss mutations not requiring gene exchange.

Our case study does not suit into the classical system of “species pairs” by Poelt (1970). The strictly sexual species of *Cetrelia* have limited distributions in eastern Asia, and they are generally infrequent or even very rare in their habitats (Randlane and Saag, 2004). Our species set mostly consisted of the more widespread “secondary species” with various vegetative reproductive structures, while truly “primary”, usually apotheciate taxa were represented only by one species, *C. sanguinea*. Therefore, we cannot dispute whether the secondary species are derived from the “primary species” or not in the genus *Cetrelia*. Still, our results showed that the production of vegetative reproductive structures had emerged in several groups independently, while secondary metabolites had each emerged only once or twice over the evolutionary history in *Cetrelia*. Similar plasticity of reproductive mode has been demonstrated also in other lichenized genera, for example in *Porpidia*, where transitions between the presence and absence of vegetative reproduction occurred several times and independently of each other (Buschbom and Barker, 2006).

We conclude by noting that the significance of chemical and reproductive characters is not the same in evolution of different groups of lichenized fungi. In several genera within Parmeliaceae, e.g. in *Bryoria* (Boluda et al., 2019), *Pseudevernia* (Ferencova et al., 2010) or *Usnea* (Mark et al., 2016), it has been shown that chemotypes may represent merely infraspecific phenotypic variation, while in the most recent study about *Usnea cornuta* aggregate several strongly supported lineages correlated with the medullary chemistry (da Cruz Lima Gerlach et al., 2018). We demonstrated that in *Cetrelia* chemical characters showed significantly higher values of consistency compared to those of the reproduction

characters. As lichen chemistry is clearly concordant with phylogenetic lineages in this genus, chemical characters could be useful as proxies for identifying independently evolving lineages and, therefore, accurate secondary metabolite identification is essential for the correct species identification in *Cetrelia*. This applies also to the widely distributed sorediate morphotype, where the chemically different species *C. cetrarioides*, *C. chicitae*, *C. monachorum*, and *C. olivetorum* are difficult or impossible for the unpracticed eye to distinguish only by morphological characters (Obermayer and Mayrhofer, 2007), but are clearly separable using TLC.

### Conflicts of interest

The authors declare no conflict of interest. The authors alone are responsible for the content and for writing the paper.

### Acknowledgements

This study was funded by the Estonian Research Council (grant PUT1017 to TR). We thank all collectors of the specimens, and two anonymous reviewers for constructive criticism. Dr. Rebecca Yahr, Royal Botanic Garden Edinburgh, and Anders Nordin, Uppsala University, are acknowledged for revising the language. GT is grateful to Dr. Akira Mori, Yokohama National University, for arranging collecting permits in Hokkaido, Japan 2010. Korean samples were obtained from the Korea Lichen and Allied Bioresource Center (KoLABIC), Suncheon National University.

### Appendix A. Supplementary data

Supplementary data to this article can be found online at <https://doi.org/10.1016/j.funbio.2018.11.013>.

### References

- Altmann, S., Leavitt, S.D., Goward, T., Nelsen, M.P., Lumbsch, H.T., 2014. How do you solve a problem like *Letharia*? A new look at cryptic species in lichen-forming fungi using Bayesian clustering and SNPs from multilocus sequence data. *PLoS One* 9, e97556. <https://doi.org/10.1371/journal.pone.0097556>.
- Altschul, S.F., Gish, W., Miller, W., Myers, E.W., Lipman, D.J., 1990. Basic local alignment search tool. *J. Mol. Biol.* 215, 403–410.
- Amo de Paz, G., Cubas, P., Divakar, P.K., Lumbsch, H.T., Crespo, A., 2011. Origin and diversification of major clades in parmelioid lichens (Parmeliaceae, Ascomycota) during the Paleogene inferred by Bayesian analysis. *PLoS One* 6, e28161. <https://doi.org/10.1371/journal.pone.0028161>.
- Barbero, M., Etayo, J., Gómez-Bolea, A., 1995. Chemotypes of *Cetrelia cetrarioides* s.l. (Lichenes) in the Iberian Peninsula. *Cryptogam. Bot.* 5, 28–30.
- Boluda, C.G., Hawksworth, D.L., Divakar, P.K., Crespo, A., Rico, V.J., 2016. Microchemical and molecular investigations reveal *Pseudophebe* species as cryptic with an environmentally modified morphology. *Lichenologist* 48, 527–543.
- Boluda, C.G., Rico, V.J., Divakar, P.K., Nadyeina, O., Myllys, L., McMullin, R.T., Zamora, J.C., Scheidegger, C., Hawksworth, D.L., 2019. Evaluating methodologies for species delimitation: the mismatch between phenotypes and genotypes in lichenized fungi (*Bryoria* sect. *Implexae*, Parmeliaceae). *Persoonia* 42, 75–100.
- Bouckaert, R., Heled, J., Kühnert, D., Vaughan, T., Wu, C.-H., Xie, D., et al., 2014. BEAST 2: a software platform for Bayesian evolutionary analysis. *PLoS Comput. Biol.* 10 (4), e1003537.
- Bowler, P.A., Rundel, P.W., 1975. Reproductive strategies in lichens. *Bot. J. Linn. Soc.* 70, 325–340.
- Buschbom, J., Barker, D., 2006. Evolutionary history of vegetative reproduction in *Porpidia* s.l. (Lichen-forming Ascomycota). *Syst. Biol.* 55, 471–484.
- Carstens, B.C., Pelletier, T.A., Reid, N.M., Satler, J.D., 2013. How to fail at species delimitation. *Mol. Ecol.* 22, 4369–4383.
- Cestaro, L., Tønsgberg, T., Muggia, L., 2016. Phylogenetic data and chemical traits characterize a new species in the lichen genus *Tephromela*. *Herzogia* 29, 383–402.
- Clerc, P., 2004. Les champignons lichénisés de Suisse. *Cryptogam. Helv.* 19, 1–320.
- Crespo, A., Kauff, F., Divakar, P.K., del Prado, R., Pérez-Ortega, S., de Paz, G.A., Ferencova, Z., Blanco, O., Roca-Valiente, B., Núñez-Zapata, J., et al., 2010. Phylogenetic generic classification of parmelioid lichens (Parmeliaceae, Ascomycota) based on molecular, morphological and chemical evidence. *Taxon* 59, 1735–1753.
- Crespo, A., Lumbsch, H.T., Mattsson, J.-E., Blanco, O., Divakar, P.K., Articus, K., Wiklund, E., Bawingan, P.A., Wedin, M., 2007. Testing morphology-based hypotheses of phylogenetic relationships in Parmeliaceae (Ascomycota) using three ribosomal markers and the nuclear RPB1 gene. *Mol. Phylogenet. Evol.* 44, 812–824.
- Crespo, A., Pérez-Ortega, S., 2009. Cryptic species and species pairs in lichens: a discussion on the relationship between molecular phylogenies and morphological characters. *Anales del Jardín Botánico de Madrid* 66S1, 71–81.
- Culberson, C.F., 1972. Improved conditions and new data for the identification of lichen products by a standardized thin-layer chromatographic method. *J. Chromatogr.* 72, 113–125.
- Culberson, C.F., Culberson, W.L., 1976. Chemosyndromic variation in lichens. *Syst. Bot.* 1, 325–339.
- Culberson, W.L., Culberson, C.F., 1968. The lichen genera *Cetrelia* and *Platismatia* (Parmeliaceae). *Contrib. U. S. Natl. Herb.* 34, 449–558.
- Culberson, C.F., Johnson, A., 1976. A standardized two-dimensional thin-layer chromatographic method for lichen products. *J. Chromatogr.* 128, 253–259.
- Cummings, M.P., Neel, M.C., Shaw, K.L., 2008. A genealogical approach to quantifying lineage divergence. *Evolution* 62, 2411–2422.
- da Cruz Lima Gerlach, A., Toprak, Z., Naciri, Y., Araujo Caviro, E., Mara Borges da Silveira, R., Clerc, P., 2018. New insights into the *Usnea cornuta* aggregate (Parmeliaceae, lichenized Ascomycota): molecular analysis reveals high genetic diversity correlated with chemistry. *Mol. Phylogenet. Evol.* <https://doi.org/10.1016/j.ympev.2018.10.035>.
- Divakar, P.K., Crespo, A., Wedin, M., Leavitt, S.D., Hawksworth, D.L., Myllys, L., McCune, B., Randle, T., Bjerke, J.W., Ohmura, Y., et al., 2015. Evolution of complex symbiotic relationships in a morphologically derived family of lichen-forming fungi. *New Phytol.* 208, 1217–1226.
- Divakar, P.K., Crespo, A., Kraichak, E., Leavitt, S.D., Singh, G., Schmitt, I., Lumbsch, H.T., 2017. Using a temporal phylogenetic method to harmonize family- and genus-level classification in the largest clade of lichen-forming fungi. *Fungal Divers.* 84, 101–117.
- Divakar, P.K., Kauff, F., Crespo, A., Leavitt, S.D., Lumbsch, H.T., 2013. Understanding phenotypical character evolution in parmelioid lichenized fungi (Parmeliaceae, Ascomycota). *PLoS One* 8 (11), e83115. <https://doi.org/10.1371/journal.pone.0083115>.
- Drummond, A.J., Suchard, M.A., Xie, D., Rambaut, A., 2012. Bayesian phylogenetics with BEAUti and the BEAST 1.7. *Mol. Biol. Evol.* 29, 1969–1973.
- Elix, J.A., Stocker-Wörgötter, E., 2008. Biochemistry and secondary metabolites. In: Nash III, T.H. (Ed.), *Lichen Biology*. Cambridge University Press, Cambridge, pp. 104–133. <https://doi.org/10.1017/CBO9780511790478.008>.
- Ferencova, Z., Del Prado, R., Pérez-Vargas, I., Hernández-Padrón, C., Crespo, A., 2010. A discussion about reproductive modes of *Pseudevernia furfuracea* based on phylogenetic data. *Lichenologist* 42, 449–460.
- Gardes, M., Bruns, T.D., 1993. ITS primers with enhanced specificity for basidiomycetes – application to the identification of mycorrhizae and rusts. *Mol. Ecol.* 2, 113–118.
- Gilbert, O.L., Purvis, O.W., 2009. *Cetrelia* W.L. Culb. And C.F. Culb. (1968). In: Smith, C.W., Aptroot, A., Coppins, B.J., Fletcher, A., Gilbert, O.L., James, P.W., Wolseley, P.A. (Eds.), *The Lichens of Great Britain and Ireland*. The British Lichen Society, London, pp. 296–297.
- Heled, J., Drummond, A.J., 2010. Bayesian inference of species trees from multilocus data. *Mol. Biol. Evol.* 27, 570–580.
- Jones, G.R., 2015. STACEY: Species Delimitation and Phylogeny Estimation Under the Multispecies Coalescent. <https://doi.org/10.1101/010199>. Preprint in bioRxiv.org.
- Jones, G., Zeynep, A., Oxelman, B., 2014. DISSECT: an assignment-free Bayesian discovery method for species delimitation under the multispecies coalescent. *Bioinformatics* 31, 991–998.
- Kass, R.E., Raftery, A.E., 1995. Bayes factors. *J. Am. Stat. Assoc.* 90 (430), 773–795.
- Katoh, K., Standley, D.M., 2013. MAFFT multiple sequence alignment software version 7: improvements in performance and usability. *Mol. Biol. Evol.* 30, 772–780.
- Katoh, K., Toh, H., 2008. Recent developments in the MAFFT multiple sequence alignment program. *Briefings Bioinf.* 9, 286–298.
- Kearse, M., Moir, R., Wilson, A., Stones-Havas, S., Cheung, M., Sturrock, S., Buxton, S., Cooper, A., Markowitz, S., Duran, C., et al., 2012. Geneious Basic: an integrated and extendable desktop software platform for the organization and analysis of sequence data. *Bioinformatics* 28, 1647–1649.
- Kukwa, M., Motiejūnaitė, J., 2010. Revision of the genera *Cetrelia* and *Punctelia* (Lecanorales, Ascomycota) in Lithuania, with implications for their conservation. *Herzogia* 25, 5–14.
- Lanfear, R., Calcott, B., Ho, S.Y.W., Guindon, S., 2012. PartitionFinder: combined selection of partitioning schemes and substitution models for phylogenetic analyses. *Mol. Biol. Evol.* 29, 1695–1701.
- Leavitt, S.D., Divakar, P.K., Ohmura, Y., Wang, L.-S., Esslinger, T.L., Lumbsch, H.T., 2015. Who's getting around? Assessing species diversity and phylogeography in the widely distributed lichen-forming fungal genus *Montanelia* (Parmeliaceae, Ascomycota). *Mol. Phylogenet. Evol.* 90, 85–96.
- Leavitt, S.D., Esslinger, T.L., Divakar, P.K., Crespo, A., Lumbsch, H.T., 2016. Hidden diversity before our eyes: delimiting and describing cryptic lichen-forming fungal species in camouflage lichens (Parmeliaceae, Ascomycota). *Fungal Biol.* 120, 1374–1391.
- Leavitt, S.D., Fankhauser, J.D., Leavitt, D.H., Porter, L.D., Johnson, L.A., St Clair, L.L., 2011b. Complex patterns of speciation in cosmopolitan "rock posy" lichens – discovering and delimiting cryptic fungal species in the lichen-forming *Rhizoplaca melanophthalma* species-complex (Lecanoraceae, Ascomycota). *Mol. Phylogenet. Evol.* 59, 587–602.

- Leavitt, S.D., Fernández-Mendoza, F., Pérez-Ortega, S., Sohrabi, M., Divakar, P.K., Lumbsch, H.T., St Clair, L.L., 2013a. DNA barcode identification of lichen-forming fungal species in the *Rhizoplaca melanophthalma* species-complex (Lecanorales, Lecanoraceae), including five new species. *Mycology* 7, 1–22. <https://doi.org/10.3897/mycokeys.7.4508>.
- Leavitt, S.D., Johnson, L.A., Goward, T., St Clair, L.L., 2011a. Species delimitation in taxonomically difficult lichen-forming fungi: an example from morphologically and chemically diverse *Xanthoparmelia* (Parmeliaceae) in North America. *Mol. Phylogenet. Evol.* 60, 317–332.
- Leavitt, S.D., Lumbsch, H.T., Stenroos, S., St Clair, L.L., 2013b. Pleistocene speciation in North American lichenized fungi and the impact of alternative species circumscriptions and rates of molecular evolution on divergence estimates. *PLoS One* 8, e85240. <https://doi.org/10.1371/journal.pone.0085240>.
- Lindblom, L., Ekman, S., 2006. Genetic variation and population differentiation in the lichen-forming ascomycete *Xanthoria parietina* on the island Storfosna, central Norway. *Mol. Ecol.* 15, 1545–1559.
- Lohtander, K., Myllys, L., Sundin, R., Källersjö, M., Tehler, A., 1998. The species pair concept in the lichen *Dendrographa leucophaea* (Arthoniales): analyses based on ITS sequences. *Bryologist* 101, 404–411.
- Lücking, R., Hodkinson, B.P., Leavitt, S.D., 2017. The 2016 classification of lichenized fungi in the Ascomycota and Basidiomycota – approaching one thousand genera. *Bryologist* 119, 361–416.
- Lumbsch, H.T., 1998. The use of metabolic data in lichenology at the species and subspecific levels. *Lichenologist* 30, 357–367.
- Lumbsch, H.T., Leavitt, S.D., 2011. Goodbye morphology? A paradigm shift in the delimitation of species in lichenized fungi. *Fungal Divers.* 50, 59–72.
- Lumbsch, H.T., Schmitt, I., Barker, D., Pagel, M., 2006. Evolution of morphological and chemical characters in the lichen-forming fungal family Pertusariaceae. *Biol. J. Linn. Soc.* 89, 615–626.
- Luo, H., Wei, X.L., Ha, K.S., Koh, Y.J., Hur, J.-S., 2007. Taxonomic study on the lichen genus *Cetrelia* (Lecanorales, Ascomycota) in South Korea. *Mycobiology* 35, 117–123.
- Maddison, W.P., 1997. Gene trees in species trees. *Syst. Biol.* 46, 523–536.
- Maddison, W.P., Maddison, D.R., 2017. Mesquite: a Modular System for Evolutionary Analysis. Version 3.2. <http://mesquiteproject.org>.
- Mark, K., Saag, L., Leavitt, S.D., Will-Wolf, S., Nelsen, M.P., Törra, T., Saag, A., Randlane, T., Lumbsch, H.T., 2016. Evaluation of traditionally circumscribed species in the lichen-forming genus *Usnea*, section *Usnea* (Parmeliaceae, Ascomycota) using a six-locus dataset. *Org. Divers. Evol.* 16, 497–524.
- Matheny, P.B., Liu, Y.J., Ammirati, J.F., Hall, B.D., 2002. Using RPBI sequences to improve phylogenetic inference among mushrooms (*Inocybe*, Agaricales). *Am. J. Bot.* 89, 688–698.
- Miller, M.A., Pfeiffer, W., Schwartz, T., 2010. Creating the CIPRES science gateway for inference of large phylogenetic trees. In: Gateway Computing Environments Workshop (GCE), 2010. IEEE, New Orleans, LA, pp. 1–8. <https://doi.org/10.1109/GCE.2010.5676129>.
- Mishra, G.K., Upreti, D.K., 2015. The lichen genus *Cetrelia* (Parmeliaceae, Ascomycota) in India. *Phytotaxa* 236, 201–214.
- Molina, M.C., Divakar, P.K., Millanes, A.M., Sánchez, E., Del-Prado, R., Hawksworth, D., Crespo, A., 2011. *Parmelia sulcata* (Ascomycota: Parmeliaceae), a sympatric monophyletic species complex. *Lichenologist* 43, 585–601.
- Myllys, L., Lohtander, K., Källersjö, M., Tehler, A., 1999. Sequence insertions and ITS data provide congruent information on *Roccella canariensis* and *R. tuberculata* (Arthoniales, Euascomycetes) phylogeny. *Mol. Phylogenet. Evol.* 12, 295–309.
- Nash III, T.H., 2008. Lichen Biology, second ed. Cambridge University Press, Cambridge, p. 502.
- Obermayer, W., Mayrhofer, H., 2007. Hunting for *Cetrelia chictae* (lichenized ascomycetes) in the eastern European Alps. *Phyton (Horn Austria)* 47, 231–290.
- Orange, A., James, P.W., White, F.J., 2001. Microchemical Methods for the Identification of Lichens. British Lichen Society, London.
- Otnyukova, T.N., Stepanov, N.V., Elix, J.A., 2009. Three new species of Parmeliaceae (Ascomycota) from Siberia. *Mycotaxon* 108, 249–256.
- Pagel, M., Meade, A., 2006. Bayesian analysis of correlated evolution of discrete characters by reversible-jump Markov chain Monte Carlo. *Am. Nat.* 167 (6), 808–825.
- Pagel, M., Meade, A., Barker, D., 2004. Bayesian estimation of ancestral character states on phylogenies. *Syst. Biol.* 53 (5), 673–684.
- Pino-Bodas, R., Martín, M., Burgaz, A., 2012. *Cladonia suburgida* and *C. iberica* (Cladoniaceae) form a single, morphologically and chemically polymorphic species. *Mycol. Prog.* 11, 269–278. <https://doi.org/10.1007/s11557-011-0746-1>.
- Pizarro, D., Divakar, P.K., Grewe, F., Leavitt, S.D., Huang, J.-P., Dal Grande, F., Schmitt, I., Wedin, M., Crespo, A., Lumbsch, H.T., 2018. Phylogenomic analysis of 2556 single-copy protein-coding genes resolves most evolutionary relationships for the major clades in the most diverse group of lichen-forming fungi. *Fungal Divers.* <https://doi.org/10.1007/s13225-018-0407-7>.
- Poelt, J., 1970. Das Konzept der Artenpaare bei den Flechten. *Vorträge aus dem Gesamtgebiet der Botanik. Neue Folge* 4, 187–198.
- R Core Team, 2014. R: a Language and Environment for Statistical Computing. R Foundation for Statistical Computing, Vienna, Austria. <http://www.R-project.org>.
- Rambaut, A., 2009. FigTree. Institute of Evolutionary Biology, University of Edinburgh, Edinburgh. <http://tree.bio.ed.ac.uk/software/figtree>.
- Rambaut, A., Drummond, A., 2007. Tracer. <http://beast.bio.ed.ac.uk/Tracer>.
- Rambaut, A., Drummond, A., 2012a. LogCombiner. <http://beast.bio.ed.ac.uk>.
- Rambaut, A., Drummond, A., 2012b. TreeAnnotator. <http://beast.bio.ed.ac.uk>.
- Randlane, T., Saag, A., 1991. Chemical and morphological variation in the genus *Cetrelia* in the Soviet Union. *Lichenologist* 23, 113–126.
- Randlane, T., Saag, A., 2004. Distribution patterns of some primary and secondary cetrarioid species. *Symb. Bot. Ups.* 34 (1), 359–376.
- Randlane, T., Saag, A., Thell, A., 1997. A second updated world list of cetrarioid lichens. *Bryologist* 100, 109–122.
- Randlane, T., Saag, A., Thell, A., Ahti, T., 2013. Third world list of cetrarioid lichens – in a new databased form, with amended phylogenetic and type information. *Cryptog. Mycol.* 34, 79–94.
- Saag, L., Mark, K., Saag, A., Randlane, T., 2014. Species delimitation in the lichenized fungal genus *Vulpicida* (Parmeliaceae, Ascomycota) using gene concatenation and coalescent-based species tree approaches. *Am. J. Bot.* 101, 2169–2182.
- Santesson, R., Moberg, R., Nordin, A., Tønberg, T., Vitikainen, O., 2004. Lichen-forming and Lichenicolous Fungi of Fennoscandia. Museum of Evolution, Uppsala University.
- Schmitt, I., Crespo, A., Divakar, P.K., Fankhauser, J.D., Herman-Sackett, E., Kalb, K., Nelsen, M.P., Nelso, N.A., Rivas-Plata, E., Shimp, A.D., et al., 2009. New primers for promising single-copy genes in fungal phylogenetics and systematics. *Persoonia* 23, 35–40.
- Stamatakis, A., 2006. RAXML-VI-HPC: maximum likelihood-based phylogenetic analyses with thousands of taxa and mixed models. *Bioinformatics* 22, 2688–2690.
- Stamatakis, A., Hoover, P., Rougemont, J., 2008. A rapid bootstrap algorithm for the RAXML Web servers. *Syst. Biol.* 57, 758–771.
- Steinová, J., Stenroos, A., Grube, M., Škaloud, P., 2013. Genetic diversity and species delimitation of the zeorin-containing red-fruited *Cladonia* species (lichenized Ascomycota) assessed with ITS rDNA and  $\beta$ -tubulin data. *Lichenologist* 45, 665–684.
- Stocker-Wörgötter, E., Elix, J.A., Grube, M., 2004. Secondary chemistry of lichen-forming fungi: chemosyndromic variation and DNA-analyses of cultures and chemotypes in the *Ramalina farinacea* complex. *Bryologist* 107, 152–162.
- Sukumaran, J., Knowles, L.L., 2017. Multispecies coalescent delimits structure, not species. *Proc. Natl. Acad. Sci. Unit. States Am.* 114 (7), 1607–1612.
- Timsina, B., Hausner, G., Piercey-Normore, M.D., 2014. Evolution of ketosynthase domains of polyketide synthase genes in the *Cladonia chlorophaea* species complex (Cladoniaceae). *Fungal Biol.* 118, 896–909.
- Tripp, E., 2016. Is a sexual reproduction an evolutionary dead end in lichens? *Lichenologist* 48, 559–580.
- Velmalá, S., Myllys, L., Goward, T., Holien, H., Halonen, P., 2014. Taxonomy of *Bryoria* section *Implexae* (Parmeliaceae, Lecanoromycetes) in North America and Europe, based on chemical, morphological and molecular data. *Ann. Bot. Fenn.* 51, 345–371.
- Wedin, M., Westberg, M., Crewe, A.T., Tehler, A., Purvis, O.W., 2009. Species delimitation and evolution of metal bioaccumulation in the lichenized *Acarospora smaragdula* (Ascomycota, Fungi) complex. *Cladistics* 25, 161–172.
- White, T.J., Bruns, T., Lee, S., Taylor, J.W., 1990. Amplification and direct sequencing of fungal ribosomal RNA genes for phylogenetics. In: Innis, M.A., Gelfand, D.H., Sninsky, J.J., White, T.J. (Eds.), PCR Protocols: a Guide to Methods and Applications. Academic Press, New York, pp. 315–322.
- Wiens, J.J., 1998. Combining data sets with different phylogenetic histories. *Syst. Biol.* 47, 568–581.
- Wirth, V., Hauck, M., Schultz, M., 2013. Die Flechten Deutschlands. Band 1. Ulmer, Stuttgart.
- Wirtz, N., Printzen, C., Lumbsch, H.T., 2008. The delimitation of Antarctic and bipolar species of neuropogonoid *Usnea* (Ascomycota, Lecanorales): a cohesion approach of species recognition for the *Usnea perpusilla* complex. *Mycol. Res.* 112, 472–484.
- Xie, W., Lewis, P.O., Fan, Y., Kuo, L., Chen, M.H., 2011. Improving marginal likelihood estimation for Bayesian phylogenetic model selection. *Syst. Biol.* 60 (2), 150–160.
- Yang, Z., Rannala, B., 2010. Bayesian species delimitation using multilocus sequence data. *Proc. Natl. Acad. Sci. Unit. States Am.* 107 (20), 9264–9269.
- Yang, Z., Rannala, B., 2014. Unguided species delimitation using DNA sequence data from multiple loci. *Mol. Biol. Evol.* 31 (12), 3125–3135.